

---

Doctoral Dissertations

Student Theses and Dissertations

---

Spring 2015

## Detection and recognition of R/F devices based on their unintended electromagnetic emissions using stochastic and computational intelligence methods

Shikhar Prasad Acharya

Follow this and additional works at: [https://scholarsmine.mst.edu/doctoral\\_dissertations](https://scholarsmine.mst.edu/doctoral_dissertations)

 Part of the [Computer Sciences Commons](#), [Electrical and Computer Engineering Commons](#), and the [Operations Research, Systems Engineering and Industrial Engineering Commons](#)

**Department: Engineering Management and Systems Engineering**

---

### Recommended Citation

Acharya, Shikhar Prasad, "Detection and recognition of R/F devices based on their unintended electromagnetic emissions using stochastic and computational intelligence methods" (2015). *Doctoral Dissertations*. 2373.

[https://scholarsmine.mst.edu/doctoral\\_dissertations/2373](https://scholarsmine.mst.edu/doctoral_dissertations/2373)

This thesis is brought to you by Scholars' Mine, a service of the Missouri S&T Library and Learning Resources. This work is protected by U. S. Copyright Law. Unauthorized use including reproduction for redistribution requires the permission of the copyright holder. For more information, please contact [scholarsmine@mst.edu](mailto:scholarsmine@mst.edu).

DETECTION AND RECOGNITION OF R/F DEVICES BASED ON THEIR  
UNINTENDED ELECTROMAGNETIC EMISSIONS USING STOCHASTIC  
AND COMPUTATIONAL INTELLIGENCE METHODS

by

SHIKHAR PRASAD ACHARYA

A DISSERTATION

Presented to the Faculty of the Graduate School of the  
MISSOURI UNIVERSITY OF SCIENCE AND TECHNOLOGY

In Partial Fulfillment of the Requirements for the Degree

DOCTOR OF PHILOSOPHY

in

SYSTEMS ENGINEERING

2015

Committee Members

Dr. Ivan G. Guardiola, Advisor

Dr. Akim Adekpedjou

Dr. Steven Corns

Dr. Cihan H. Dagli

Dr. Randy H. Moss



## ABSTRACT

Radio Frequency (RF) devices produce some amount of Unintended Electromagnetic Emissions (UEEs). UEEs are generally unique to a device and can be thought of as a signature of the device. This property of uniqueness of UEEs can be used to detect and identify the device producing the emission. The problem with UEEs is that they are very low in power and are often buried deep inside the noise band which makes them difficult to detect. There are two types of UEE detection methods. The first one is called stimulated detection method where the UEEs of a device are enhanced using external stimulation signal and the detection is made based on the analysis of the enhanced stimulated signal. This method, however, is resource intensive as the generation, transmission, and reception of the stimulation signal requires hardware components. The second UEE detection method is called passive detection method where the UEE signals are not tampered with and are analyzed in its original raw form. Since the UEEs are weak in strength, the challenge with passive detection method is to measure and analyze UEEs in a noisy environment.

In order to detect and recognize RF devices through the UEE, the first step is to measure the leakage of electric signal that is emitted outside of the RF devices as UEEs. UEE samples are collected from two RF devices at three different distances of 3 feet, 6 feet and 10 feet and also for noise in a similar environment. The three methods explored in this research are Principal Components Analysis (PCA), Hidden Markov Model (HMM), and Support Vector Machine (SVM). This research studies the performance of these three algorithms for passive detection of UEEs and compares it with the performance of Neural Network (NN). The explored methods gives significant better results than existing methods and can be used as an alternative for the costly and resource intensive stimulated detection methods. One of the major application of UEE is in the detection of Improvised Explosive Devices (IEDs). Effective IED detection system for military operation should accurately perform the task of detection, localization, and direction of malicious devices. This research contributes to the detection and recognition of IED detection system by proposing models based on stochastic and computational intelligence methods. These methods proved to have promise if it can be implemented in real life with more applied research.

## ACKNOWLEDGMENTS

I would like to thank my academic advisor Dr. Ivan G. Guardiola for his continuous support. This work would not have been possible without his guidance and supervision. I would also like to thank my committee members Dr. Akim Adekpedjou, Dr. Steven Corns, Dr. Cihan Dagli, and Dr. Randy Moss for their thoughtful comments to improve the quality of this work.

I would like to thank all the members of Smart Engineering Systems Lab, especially the ones ahead of me for creating a positive and friendly work environment. My special thanks goes to Ritesh Arora for his significant contribution in collecting the UEE signal used in this work. I would also like to thank Nepali community of Rolla for making me feel at home. I am very thankful to Dr. Bonnie Bachman for accepting me as her research assistant during the summer of 2014. Many many thanks to Nancy and Tiny, my guardians in Rolla. It was my privilege to know Sashi Gurung: friend, family member, and a great human being. Frequent visits of Dilip Yogi provided me with the much needed social outings that kept me going throughout the PhD program.

My special thanks goes out to my parents Keshav Prasad Acharya and Lalita Acharya. Their love and support throughout my life was vital in one way or the other in completing this program. My younger sister Achala completed PhD ahead of me as if to tell me if I can do it, you can too.

Ideally I should not thank my daughter Juneli for this work. Her contribution, if anything, was distraction. But she is the kind of distraction that makes life worth living. My wife Shristy Bashyal Acharya has sacrificed so much for the completion of my PhD degree that her name should be somewhere in the title page. Thank you for your support and encouragement.

## TABLE OF CONTENTS

	Page
ABSTRACT .....	iii
ACKNOWLEDGMENTS .....	iv
LIST OF ILLUSTRATIONS .....	viii
LIST OF TABLES .....	x
LIST OF NOTATIONS .....	xi
 SECTION	
1. INTRODUCTION .....	1
2. UNINTENDED ELECTROMAGNETIC EMISSIONS .....	8
3. BACKGROUND .....	13
3.1. DETECTION METHODS .....	13
3.1.1 Stimulated Detection Methods .....	14
3.1.1.1 Modulation method .....	14
3.1.1.2 Long PN code method .....	14
3.1.1.3 Stagner method .....	16
3.1.2 Passive Detection Method .....	16
3.1.2.1 Matched filter method .....	16
3.1.2.2 Cascading correlation method .....	17
3.1.2.3 Hurst parameter method .....	17
3.1.2.4 Granulometric size distribution .....	18
3.2. RECOGNITION METHODS .....	19
3.2.1 Neural Networks .....	19
3.3. SUMMARY .....	20
4. METHODOLOGY .....	22
4.1. PRINCIPAL COMPONENTS ANALYSIS .....	23
4.1.1 Definition .....	28
4.1.2 UEE Detection Using PCA .....	30
4.1.3 Feature Extraction .....	31
4.2. HIDDEN MARKOV MODELS .....	32
4.2.1 HMMs and UEEs .....	33

4.2.2	Definition .....	34
4.2.3	Three Problems for HMM .....	35
4.2.4	Solution to the Evaluation Problem .....	36
4.2.5	Solution to the Decoding Problem .....	37
4.2.6	Solution to the Learning Problem .....	38
4.2.7	Data Collection and Preprocessing .....	38
4.2.8	Feature Extraction .....	38
4.2.9	Training.....	39
4.2.10	Assumptions of HMM .....	40
4.3.	SUPPORT VECTOR MACHINE.....	42
4.4.	NEURAL NETWORKS .....	44
5.	RESULTS .....	48
5.1.	DETECTION .....	48
5.1.1	Principal Components Analysis .....	48
5.1.2	Hidden Markov Models .....	54
5.1.3	Support Vector Machine.....	55
5.1.4	Neural Networks .....	56
5.2.	RECOGNITION.....	56
5.2.1	Principal Components Analysis .....	57
5.2.2	Hidden Markov Models .....	57
5.2.3	Support Vector Machine.....	58
5.2.4	Neural Networks .....	59
6.	CONCLUSION AND FUTURE WORKS .....	60
APPENDICES		
A.	Matlab Code for UEE Data Processing.....	64
B.	Matlab Code for PCA calucation of UEEs .....	72
C.	R code for Baum Welch algorithm .....	74
D.	R code for Support Vector Machine.....	76
E.	Data segment for D1 at 3 feet .....	79
F.	Data segment for D1 at 6 feet .....	81
G.	Data segment for D1 at 10 feet.....	83
H.	Data segment for D2 at 3 feet .....	85
I.	Data segment for D2 at 6 feet .....	87

J. Data segment for D2 at 10 feet .....	89
K. Data segment for Noise .....	91
BIBLIOGRAPHY .....	93
VITA .....	100

## LIST OF ILLUSTRATIONS

Figure	Page
1.1 Mobile Cellular Subscriptions in US (per 100 people) .....	2
1.2 Improvised Explosive Device (adapted from <i>commons.wikimedia.org</i> )...	5
1.3 Coalition Forces Death in Afghanistan .....	5
2.1 Unintended Electromagnetic Emission from a walkie talkie radio .....	9
2.2 UEE and Noise Signal .....	10
2.3 Local Oscillator.....	11
2.4 Block Diagram of Superheterodyne Receiver .....	11
2.5 Block Diagram of Super Regenerative Receiver .....	11
4.1 Number of Observations Required to Estimate the Standard Multivariate Normal Density Function such that the Mean Square Error is less than 0.1	23
4.2 PCA of White Gaussian Noise .....	25
4.3 PCA of Square Signals .....	26
4.4 PCA of Triangle Signals .....	27
4.5 PCA of Sawtooth Signals .....	27
4.6 Percentage of Variation Explained by Each of the Top 10 PCs of Noise, Square Signal, Triangle Signal, and Sawtooth Signal .....	28
4.7 Experimental Setup for Data Collection.....	30
4.8 Application of PCA for UEE detection.....	31
4.9 Basic Structure of Hidden Markov Model .....	33
4.10 Hidden Markov Model for UEE Identification .....	34
4.11 Signal Identification Process.....	35
4.12 Ergodic Markov Chain .....	39
4.13 Support Vector Machine .....	43
4.14 Neural Networks.....	46
5.1 Average Contribution of Top 10 PCs for Devices and Noise .....	50
5.2 Principal Components of Noise.....	51
5.3 Principal Components of Device 1 at 3 feet .....	51

5.4	Principal Components of Device 1 at 6 feet .....	51
5.5	Principal Components of Device 1 at 10 feet .....	52
5.6	Principal Components of Device 2 at 3 feet .....	52
5.7	Principal Components of Device 2 at 6 feet .....	52
5.8	Principal Components of Device 2 at 10 feet .....	53

## LIST OF TABLES

Table	Page
1.1 Percentage of Fatalities of Coalition Forces from 2001 to 2013 Caused by IED .....	5
3.1 Detection Range for Long PN Code Method .....	15
4.1 Distribution of Variation Explained by Principal Components .....	26
4.2 Chi Square Test for First Order Markov Chain .....	41
5.1 Cumulative Contribution of Top 10 Principal Components (PC) .....	49
5.2 Average Contribution of Top 10 PCs for Devices and Noise .....	50
5.3 Decision Table to Detect UEE .....	50
5.4 Device Detection using HMM .....	54
5.5 Device Detection using SVM .....	55
5.6 Device Detection using NN .....	56
5.7 Total Variation Explained by top 2, 5, and 10 PCs of Two Devices .....	57
5.8 Device Recognition using HMM .....	58
5.9 Device Recognition using SVM .....	58
5.10 Device Recognition using NN .....	59

## LIST OF NOTATIONS

- $\mathbf{A}_p$  input data for PCA
- $\mathbf{X}$  m-dimensional input vector
- $l$  number of principal components
- $\mathbf{Q}$  orthogonal transformation matrix of  $\mathbf{X}$
- $\mathbf{X}_r$  reduced  $\mathbf{X}$  after PCA
- $\mathbf{q}$  unit vector
- $\mathbf{R}$  correlation matrix of  $\mathbf{X}$
- $\mathbf{a}$  set of projection
- $\lambda_p$  eigenvalues of correlation matrix  $\mathbf{R}$
- $P_r$  percentage variation of individual Principal Components
- $\mathbf{N}$  number of states of HMM
- $\mathbf{S}_N$  individual states of HMM
- $\mathbf{T}$  number of observations of HMM
- $\mathbf{O}_T$  individual observations of HMM
- $\mathbf{A}$  transition probability matrix
- $\mathbf{B}$  observation probability matrix
- $\pi$  initial probability distribution
- $\rho$  margin of separation in SVM
- $\mathbf{w}$  weight vector of SVM
- $\mathbf{b}$  bias of SVM
- $\phi$  activation function of NN

## 1. INTRODUCTION

The number of wireless devices available has grown substantially during the last few decades. Nowhere is this growth more evident than in the growth of mobile/cellular phone subscribers. Figure 1.1 illustrates the increase in the number of mobile subscriptions in the United States per 100 people from 1984 to 2012 [1]. Less than 1% of the United States population had a mobile phone in 1984; eleven years later, that number had reached 10%. The number of subscribers has grown exponentially thereafter, reaching almost 100% in 2012. People use a variety of wireless devices in their daily lives. These include headphones, speakers, computer keyboards, computer mice, printers, garage door openers, and Global Positioning System (GPS) receivers. The sale of wireless devices has grown with their use. An example of this growth can be seen in the sales of GPS receivers. GPS receivers are wireless devices that can calculate the position and velocity of objects based on the signals received from the GPS satellite system [2]. There were 69 million GPS receiver units sold in 2005 alone. These sales increased to over 122 million in 2010 [4]. It is estimated that one billion GPS enabled devices will be sold in 2014 [3].

The growth of wireless technology will likely continue in the future as many non-wireless devices are currently being built to have wireless capabilities. Many traditional accessories (e.g., watches and spectacles) have some wireless features embedded within them. The use of wireless technology in jewelry has been around for decades. Common examples include an embedded microphone on a necklace and earphone in earrings [5]. Several automobile companies have begun to provide high speed 4G LTE in vehicles [6]. The tremendous growth of wireless devices has made them ubiquitous in modern society, and this growth is not expected to slow down in the immediate future.

Wireless technology has improved the quality of life in many ways. The proliferation of wireless devices has enabled people to connect and communicate with almost anyone wherever and whenever they want. For example, the Himalayan region, an

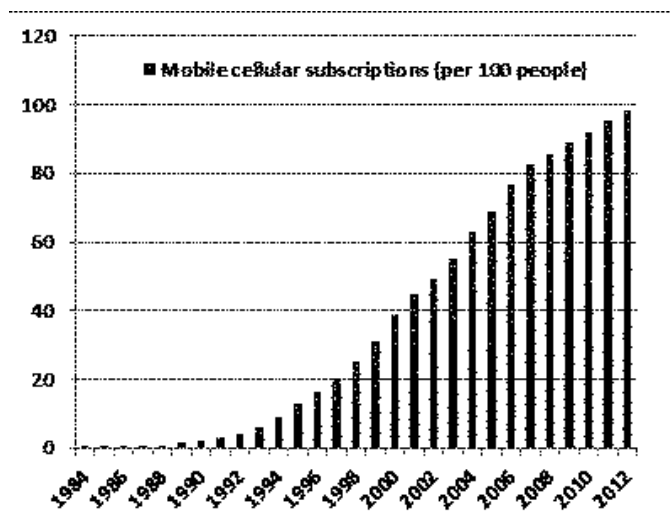


Figure 1.1 Mobile Cellular Subscriptions in US (per 100 people)

area considered one of the most remote places on the planet, is now connected to the rest of the world through wireless devices [7].

Wireless devices are incredibly useful in the relief operations during a natural disaster. Wireless devices are particularly useful during specific operations like locating, tracking, and providing immediate relief to the victims [8]. For example, after an earthquake, searching for victims beneath collapsed structure such as buildings and bridges is very risky. There is a significant risk that the rescue operation will further destabilize the structure causing more fatalities amongst trapped victims or the relief worker themselves. In this type of scenario, the robots with wireless signal transmitter makes the relief operation safer and efficient. Small robots with audio and video sensors with wireless signal transmitter can explore the remains of collapsed structures and send information about the location and condition of the victims [9] and [10].

Wireless telemedicine is another useful application of wireless technology. Wireless telemedicine is a fast and effective method to provide clinical health care to patients located at a different geographical location from the health care providers [11]. Telemedicine system generally consists of two units. The first unit is a mobile unit that is located near the patient. It transmits vital information about the patient such as electrocardiogram, pulse rate, etc. The second unit is called the consulta-

tion unit that is located with the health care expert. The consultation unit receives information from mobile unit. Based on the information received, the health care expert diagnose the medical condition of the patient and give directions for treatment. These directions are implemented by medical staff located near the mobile unit [12]. Another similar application of wireless devices in medicine includes the real time and continuous home monitoring of chronic and elderly patients [13]. Wireless technology enables the monitoring of the health condition of such patients continuously and in near real-time when the patient is at home. This reduces the medical cost of the patient as they don't have to pay for the costly medical bills of hospital stay [14]. These examples illustrates that the wireless technology has made this world a better place to live.

As the saying goes that every coin has its other side, no matter how useful wireless technology has become, there will always be some drawbacks. For example, the increasing worldwide use of wireless devices has created an extensive amount of electromagnetic pollution [15]. It is difficult to find an open area in the planet without some amount of electromagnetic radiation. It is not completely known how harmful this electromagnetic pollution is to the human health. Some preliminary studies are suggesting negative health effects of such exposure [16]. Preliminary results suggests a link between extensive usage of wireless devices cause minor health issues such as sleep depravation and headache to major health concerns like cancer [17]. Not only human beings, but plants and animals are also subjected to the negative effects of electromagnetic pollution [18]. A study by Irmak et. al (2002) observed the negative effect of electromagnetic radiation on rabbits. They observed an increase in the stress levels in the animals under study [19].

Interference is another negative consequence of electromagnetic pollution. Interference is the undesired functioning of an electronic circuit due to an unwanted external electromagnetic signal being conducted through the device [20]. Electromagnetic interference has been found to cause medical equipment malfunction [21]. Mobile phones are not allowed inside intensive care unit of hospitals as the interference of electromagnetic radiation from the mobile phone with the medical equipment

may be fatal for the patients [22]. For example, a pacemaker, which is a medical device placed in the heart of a patient to control the heart rate is prone to external interference. Interference of external electromagnetic signals have been found to alter the basic functions of the pacemaker, sometimes causing adverse effects to the patient [23]. One of the adverse effect of interference of cell phone on pacemaker is the oversensing effect (pacemaker tracking an increase in the heart-beat rate of the patient when the heart-beat rate is normal) causing the pacemaker to lower the heart-beat rate of the patient [24].

Furthermore, some places completely restrict the use of wireless devices due to security and privacy concerns. Examples of such places are customs offices and courthouses, which prohibit the use of wireless devices as these devices may be used to illegally record or interrupt the proceedings [25]. In some extreme cases, wireless devices are used as weapons to inflict physical damage to others. In such cases, it is very difficult to control or avoid the use of wireless devices. An example of such usage of wireless technology in a malicious manner is Improvised Explosive Devices (IEDs). IEDs are homemade explosive devices made from easily available, low cost and legally available raw materials such as inorganic salts and peroxides that are compounds generally found in commercially available fertilizers [26]. A picture of an IED is depicted in Figure 1.2 [27]. The picture shows an IED where a walkie talkie is connected to explosive materials through a wire. The purpose of wireless device is to remotely detonate the IED. There are two methods to detonate an IED. First, is to wire the explosive material to the RF receiver directly. A call is then made to that walkie talkie, which acts as an detonator. Secondly, a timer is set using the internal alarm of the RF receiver. The IED will detonate when the alarm is triggered [28].

IEDs were the primary cause of a large number of coalition fatalities during the Afghanistan and Iraq war. Figure 1.3 illustrates the number of coalition fatalities in Afghanistan and the number of those fatalities attributed to IEDs. It can be observed in the figure that a large number of deaths is caused by the IEDs. Table 1.1 further clarifies the fact that IEDs are the major weapons used by the terrorists against coalition forces. IEDs caused 40.75% of the total deaths of the coalition fatalities



Figure 1.2 Improvised Explosive Device (adapted from *commons.wikimedia.org*)

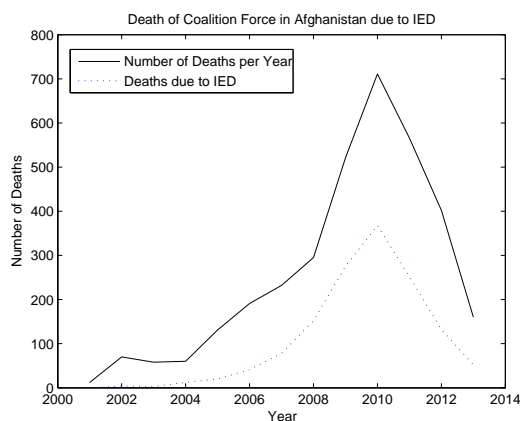


Figure 1.3 Coalition Forces Death in Afghanistan

Table 1.1 Percentage of Fatalities of Coalition Forces from 2001 to 2013 Caused by IED

Year	Fatalities due to IED
2001	0.00%
2002	5.71%
2003	5.17%
2004	20.00%
2005	15.27%
2006	21.47%
2007	33.62%
2008	51.53%
2009	52.78%
2010	51.76%
2011	44.52%
2012	32.84%
2013	32.50%

from 2001 to 2013. If it is somehow possible to detect IEDs present nearby, the number of deaths can be significantly reduced not only in Afghanistan, but in other hostile environments where this form of warfare exists. It can thus be concluded that detection and localization of RF receivers in a hostile territory could be an effective approach to reduce the number of fatalities.

One way of controlling undesired and illegal usage of wireless electronic devices

is to detect them while they are inactive. The identification and detection of wireless devices in prohibited areas will help to minimize their harmful effects and/or consequences. Security officers like a bailiff in a court room can determine if there is an illegal use of devices occurring. Army personnel can identify and locate IEDs in an area and safely deactivate it before it can cause harm. There are different methods for detecting devices. The following paragraphs discuss two of the most common device detection methods in use today: radio frequency identification (RFID) method and bug scanning method.

RFID is one of the most commonly used methods for device detection and identification. RFID is a method that enables the automatic identification of physical objects through the use of radio signals. RFID consists of two parts, which are a tag and a reader. The tag consists of a small microchip that can store information and is capable of wireless data transmission [29]. The reader can detect the tag by reading the information that is transmitted by the tag [30]. The major reason for the popularity of RFID is its low cost. RFID are used by large and well known companies and organizations such as Wal Mart, Procter and Gamble, and the United States Department of Defense in a wide variety of products, further increasing its popularity [29], [31]. One of the requirements of RFID is that the object that is to be detected has to have a unique tag. This requirement restricts the use of RFID as a device detection method in many cases. For example, to use RFID method to detect IED, the tag of the RFID has to be attached to IED, which is not possible.

Bug scanning is another common method used for the detection of electronic devices. In the bug scanning method, the device that is to be detected is exposed by an external source of strong electromagnetic radiation and the re-emitted electromagnetic radiation is analyzed for the detection process [32]. Bug scanning is capable of detecting any device that contains PN junction. A PN junction is the area of a semiconductor where two types semiconductor materials are joined together. If a PN junction is present in the electronic device, the junction will cause the stimulated signal to bounce back with its harmonics and the presence of this reflected harmonics signifies the presence of electronic devices [33]. Seguin (2009) has pointed two major

drawbacks of this method that causes serious limitations in its application for device detection. Firstly, not only PN junction, but different types of junctions including metal junctions will rectify the stimulated signal. This, in turn, increases the false positive rates of detection to an unacceptable level as even a simple metal junction such as a rusty nail will be classified as an electronic device. Secondly, the electromagnetic signals that are re-emitted are extremely weak in power. This low power signal is difficult to capture and measure [32]. The power of the re-emitted signal can be increased by using a very strong stimulation signal. However, the strong stimulation signal increases the false positive rates by interacting with many more metal junctions within surroundings. Due to these disadvantages, bug scanning methods have serious limitations in IED detection. The drawbacks of RFID method and the bug scanning methods makes those methods unsuitable for IED detection. Thus, there is a need for robust IED detection and recognition methods.

The primary purpose of Systems Engineering is to bring a system into existence that satisfies the need of the customer. Effective IED detection system for a military operation should accurately perform the tasks of detection, localization, and direction of malicious device at a long distance. This research contributes to the detection aspect of the overall IED detection system by exploring various stochastic and computational intelligence methods based on the leakage of electromagnetic signals from electronic device components. It also contributes to the passive detection approach of malicious devices by proposing methods that are capable of not only detection but also of recognition. The proposed methods has a potential of being implemented in real life applications of military operations of IED detection system.

The next section will introduce Unintended Electromagnetic Emissions (UEEs) and explain how it can be used for IED detection. It will discuss the generation and characteristics of UEE and explain the challenges associated with UEE detection and recognition.

## 2. UNINTENDED ELECTROMAGNETIC EMISSIONS

All electronic devices emit some form of electromagnetic radiation. Electronic devices with any kind of electronic circuits or which work at RF frequencies emit some amount of Unintended Electromagnetic Emissions (UEEs) [34]. These emissions are generated by the signals created by a local oscillator within an integrated circuit. As an example, a circuit diagram of a local oscillator is reproduced in Figure 2.3 [35]. In this figure,  $Q$  denotes a transistor,  $L$  denotes an inductor,  $C_1$  and  $C_2$  denotes the two capacitors, and,  $R_L$  and  $R_{EE}$  denotes the two resistors. The local oscillator emit electromagnetic signals which couple with device's antenna, connection wires, or housing of the device and are radiated outside the device as UEEs [36], [37]. An example of an UEE signal is shown in Figure 2.1. The Figure consists of amplitude in dBm plotted against 1001 data points. Each data point represent a frequency that are 20 Hz apart. The details of the data collection process for the UEE signal is explained in Section 4.1.2. An increase in the power in the UEE signal can be observed around the central frequency, which is denoted by a shadowed area with dotted lines in Figure 2.1. Figure 2.2 shows both an UEE signal and a noise signal to illustrate the difference between them. In the case of the UEE signal, a significant increase in power can be observed between 450 and 550 data points. But the difference in noise is that there are many non-significant but random increases in power within the signal trace. A consistent but significant increase in power is a feature of UEE that helps us to detect UEEs from the ambient noise. As the magnitude of increase in power in UEEs, and the range within which increase in power occurs is different for different devices, UEEs can also be used for device recognition. The challenge in UEE detection and recognition, however, is that the increase in power is low and the range within which an increase in power occurs is small. In addition, UEEs are often buried in the ambient noise band. The method of UEE detection and recognition should be robust enough to overcome these challenges.

The characteristics of the UEEs depend upon the configuration and charac-

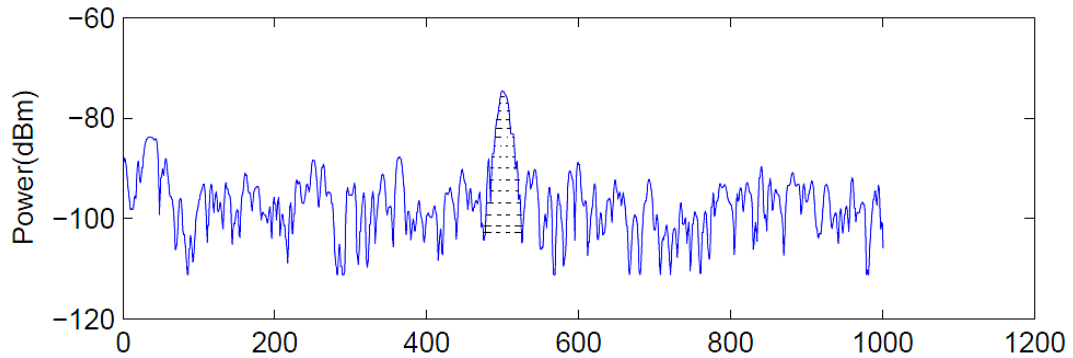


Figure 2.1 Unintended Electromagnetic Emission from a walkie talkie radio

teristics of the various components of the electronic device emitting the UEEs [38]. There always exist some differences between various internal electronics components such as resistors and transistors between different devices. The main reason of the difference between these components is due to the fact that the tolerance of the components are different for different devices. Tolerance of any component can be defined as the variation allowed for that component. For example, a  $1K \Omega$  resistor with a tolerance of 10% can be expected to measure between  $900 \Omega$  and  $1100 \Omega$  whereas a  $1K \Omega$  resistor with a tolerance of 2% can be expected to measure between  $980 \Omega$  and  $1020 \Omega$ . Let us now take the example of the oscillator illustrated in Figure 2.3. There may be different devices that use the oscillators with exactly the same circuit design as in Figure 2.3. But the characteristics of the oscillators will differ between different devices due to the operating values and the tolerances of these electronic components. Since the combination of the characteristics of these components are unique, the characteristics of the UEEs generated by these devices will also be unique. This uniqueness feature of UEEs can reveal valuable information about a particular electronic device [37]. UEEs can thus be taken as a unique signature of electronic devices that can be used for device detection and identification.

In this research, the attention is focussed on the UEEs from Radio Frequency (RF) devices. Typical RF devices have either superheterodyne or super-regenerative receivers (SRR) [39]. The superheterodyne receiver architecture was invented by Edwin Armstrong in 1918. This architecture is popular since it allows the RF signal

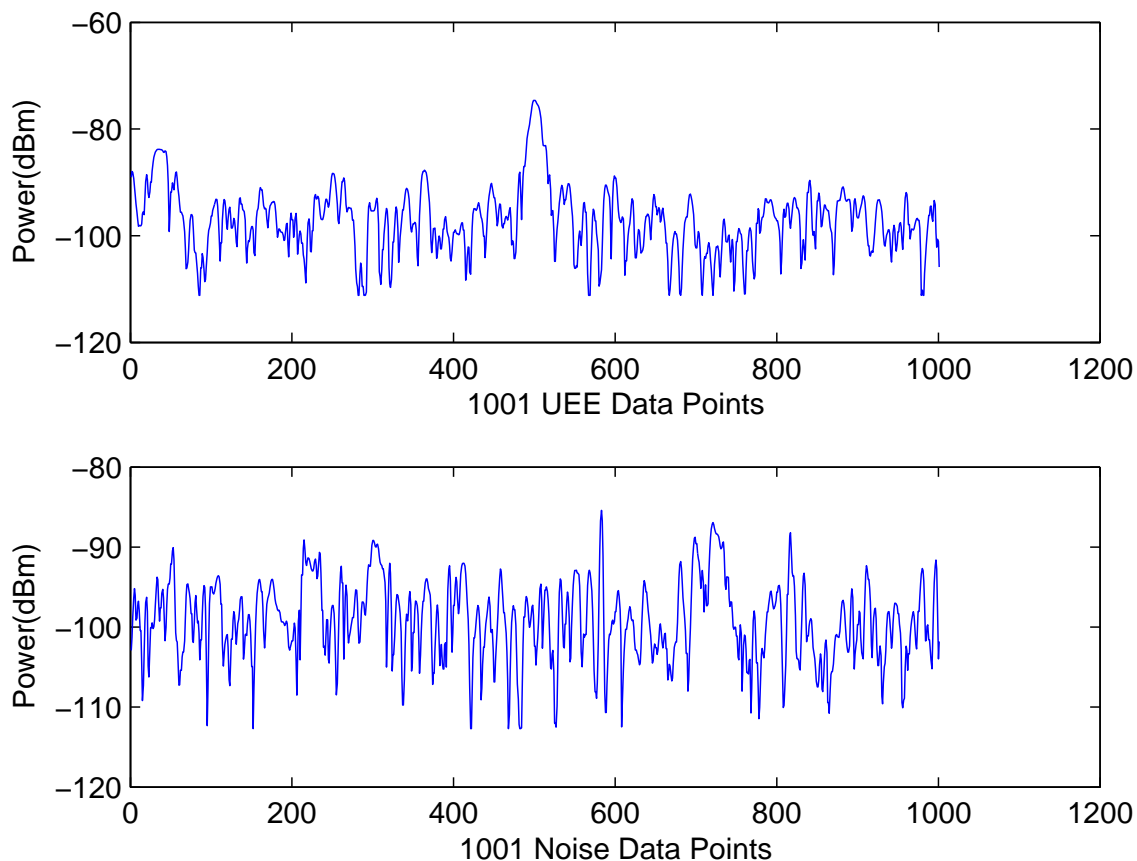


Figure 2.2 UEE and Noise Signal

to be converted down to a fixed lower Intermediate Frequency (IF), replacing a low  $Q$  tunable RF filter with a low cost high  $Q$ -IF filter [40]. A block diagram of a superheterodyne receiver is illustrated in Figure 2.4. The energy generated by the local oscillator is intended to be used only within the receiver. However, in practice, some amount of this energy usually escapes into the environment resulting in UEEs [41] [42].

As illustrated in the block diagram of a SRR in Figure 2.5, there is a feedback in the SRR which connects the output of the receiver to the input. The purpose of the quench generator is to periodically interrupt the main RF oscillation [43]. Ideally, all of the energy generated by this quench generator should be absorbed by the receiver. In reality, however, some leakage occurs in this process and some amount of energy generated by the quench generator is emitted as UEEs [39].

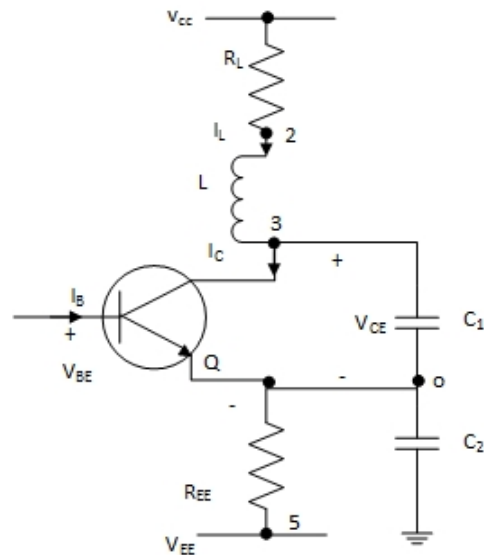


Figure 2.3 Local Oscillator

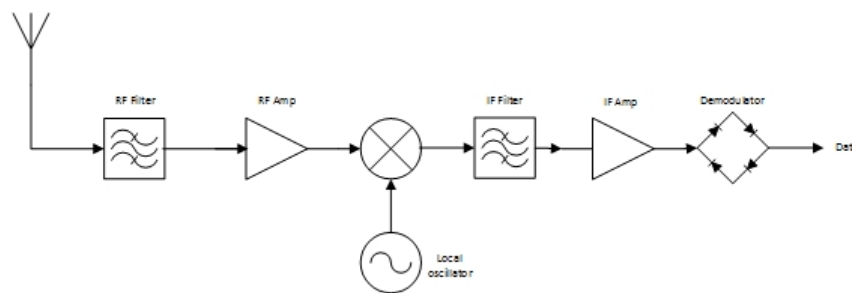


Figure 2.4 Block Diagram of Superheterodyne Receiver

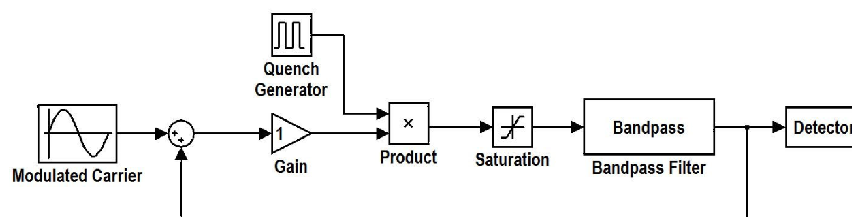


Figure 2.5 Block Diagram of Super Regenerative Receiver

Detection of RF receivers using their UEEs at a significant distance is difficult due to the high levels of ambient noise [32]. Another difficulty arises due to the fact that the power of the UEEs are weak and also varies according to the receiver model and year [40]. The challenge is to detect the low power, variable strength UEE signals

which are deeply buried within the ambient noise band. The next section will discuss some of the methods of detection of these signals found in the current literature. It will highlight the most relevant approaches to identify, detect, and recognize UEE signals from every day wireless devices.

### 3. BACKGROUND

This section discusses the most common detection and recognition methods associated with UEEs that are available in the current literature. Detection is the process of distinguishing UEEs from ambient noise in a specific frequency band, whereas, recognition is the process of distinguishing between multiple sources of UEEs in a specific frequency band. The methods of detection and recognition of UEEs can be further classified into two types: stimulated detection and passive detection.

In the stimulated detection methods, the underlying characteristics of UEE is strengthened and stabilized by an external stimulation signal. Stimulation detection method is based on the fact that the characteristics of the UEEs become more consistent when subjected to an appropriate external RF stimulation. External simulation not only improves the quality of the UEEs, but also helps in consistent receipt of the UEEs. Receiving a consistent UEEs is important in detection as UEEs are often buried in the noise band and are sometimes even below the ambient noise level. The stimulation signal increases the intensity of the low power UEE signal and also enables the steady flow of the consistent signal, thus making it easier for detection.

Unlike stimulated detection of UEEs, the UEEs in the passive detection methods are not tampered with and are analyzed in their raw form [43], [32]. The challenge of passive detection is that UEEs are low in power and it makes it difficult to detect and analyze the UEEs in a noisy environment. This section will discuss the common methods available in literature for both stimulated and passive detection and recognition of UEEs.

#### 3.1. DETECTION METHODS

For the purpose of this research, detection is defined as the the process of identifying UEEs in a specific frequency band. Moreover, detection is the process of detecting UEEs that are buried in the ambient noise and determine if there exists UEEs in a specific frequency band or not.

**3.1.1 Stimulated Detection Methods.** The three stimulated detection methods commonly found in the literature and discussed in this section are: the modulation method, the long PN code method and the Stagner method. In all of the methods discussed in this section, an external source is used to strengthen and improve the quality of the UEEs. It is necessary for the creation of external stimulus signal in all the three methods. Arrangements has also to be made for capturing and measuring the reflected signals. All these methods also require the computation of a specific threshold value to decide the presence or absence of UEEs. The threshold value is calculated based on the measurements in a semi-anechoic chamber. Semi-anechoic chamber insulates the inside of the chamber from external electromagnetic radiation to prevent interference with signals within the chamber.

**3.1.1.1 Modulation method.** In the modulation method, amplitude modulated signals are used as the stimulus signal to strengthen the UEEs from a device. This results in the characteristics of the reflected UEEs to be more consistent and enhanced, making it easier to detect the presence of the electronic device emitting the UEEs [32]. In this method, the energy of the reflected stimulated signal is predetermined in a semi anechoic chamber. The decision of whether a device is present or not is based on the comparison of correlation coefficient of the energy level of tested stimulated signal with the predetermined stimulated signal. An electronic device is considered to be detected if the correlation coefficient of the energy level of stimulated and the reflected signal is greater than a specific threshold value predetermined in the semi anechoic chamber. It is claimed in [32] that the probability of detection is increased and the probability of false alarm, which is defined as the detection of signal when it is not present, is significantly decreased as compared with passive detection method of cascading correlation. This method, however, requires many overhead operations as compared to any of the passive detection methods.

**3.1.1.2 Long PN code method.** Long Pseudo-Noise(PN) Code Method for UEE detection uses PN sequence as the stimulation signal [43]. The PN sequence is

uniformly distributed and independent periodic sequence of binary bits that repeats after a certain number of bits called the length of the PN sequence. The PN sequence appears to be random, however, they are not statistically random [44] as it repeats itself after the length of the PN sequence. In [45], Universal Software Radio Peripheral (USRP) was used for the purpose of transmitting a PN sequence and receiving the reflected stimulated UEEs. A PN sequence of a specific length was used as the stimulation signal. The reflected stimulated signal consisted of UEEs modulated with with the PN sequence. The reflected PN sequence is then correlated with the original PN sequence in the stimulated signal. A device is determined to be detected if this correlation value is larger than the previously determined threshold value. This threshold value is determined in a noiseless semi-anechoic chamber.

The range of detection is depended on the length of the PN sequence. Lower length of the PN sequence can detect device for a shorter distance but as the length of the PN sequence increases, so did the detection range [43]. This effect of an increase in detection range with an increase in the length of PN code is illustrated in Table 3.1. We can observe in Table 3.1 that when the PN sequence of 63 bits was used as stimulation signal, the detection range was 26 feet. The detection range subsequently increased to 48 feet with PN sequence of 2047 bits and to 62 feet with PN sequence of 8191 bits. Even though the Long PN Code Method increases the range of detection as compared to the modulation method, the actual accuracy of the method was not given in the research papers [43], [45].

<b>Length of PN sequence</b>	<b>Detection range</b>
63 bits	26 feet
2047 bits	48 feet
8191 bits	62 feet

Table 3.1 Detection Range for Long PN Code Method

**3.1.1.3 Stagner method.** In this stimulated detection method, the stimulated signal used is the sum of input RF and local oscillator signal [46]. Selection of stimulation signal is comparatively easier than for Modulation Method and Long Code PN Method as the restrictions for the signal is that the duration and the power should be high [46]. The experiments performed in [46] showed an improved performance over passive detection method. The disadvantage of this method is that a threshold of matched filter value has to be determined for each devices to be detected. This is required for the detection process as a detection is made when the number of matches of test signal is greater than pre-determined threshold value. Another limitation of this study is this is a theoretical study where the signals used were simulated and were not the actual signals recorded in an lab based or real world settings.

**3.1.2 Passive Detection Method.** The six passive detection methods commonly found in the literature and discussed in this section are: matched filter method, cascading correlation method, Hurst parameter method, granulometric size distribution method, and principal components analysis method. The first three methods (matched filter method, cascading correlation method, and the Hurst parameter method) are threshold based methods. These methods require the calculation of a specific threshold value in an semi-anechoic chamber to decide the presence or absence of UEEs. The last two methods (granulometric size distribution method and principal components analysis method) are not threshold based methods and thus doesn't require the overload of calculation of threshold value in a semi-anechoic chamber.

**3.1.2.1 Matched filter method.** Shaik et al. (2006) used matched filter to detect electronic devices based on their UEEs [34]. A matched filter to the signal  $s(t)$  is a linear time-invariant filter with impulse response  $h(t) = s(T-t)$ , where  $s(t)$  is assumed to be confined to the time interval  $0 \leq t \leq T$  [47]. Matched filters are linear filters that are generally used to detect signals corrupted by white Gaussian noise[41]. To identify the existence of a particular device, a matched filter is first

constructed from a given device. The signal that is to be detected is then passed through this filter. A signal is determined to be detected if the power of the output is greater than a predetermined threshold. Even though this is a noble method for detection of UEEs, the accuracy of the method decreases significantly as the distance of the source of emission increases [32]. The matched filter in [34] was constructed from the noiseless data of semi-anechoic chamber.

**3.1.2.2 Cascading correlation method.** Cascading Correlation is the process of combining different signals by iteratively correlating them together. Cascading Correlation method for UEE detection consists of characterizing a device by using specific parameters of the emissions in both time and frequency domain. The parameters are the shape, rate, and frequency content of the emissions pulses, the change in frequency content over time, and the change in emissions characteristics when subject to different noise conditions and environments [32]. An ideal pulse is then developed by iteratively cross correlating a statistically significant number of characterized pulses. The normalized pulse value is obtained after correlating all the pulses and is called the "ideal pulse". The emission that is to be determined is then correlated to the constructed ideal pulse. If the value is above a certain threshold, then the emission is determined to be from the corresponding device that generated the ideal pulse [32]. Experimental results of this method showed that this method can identify the presence of UEEs with an area under the Receiver Operating Characteristic (ROC) curve of 98% at 3 meters. The primary drawback of this method is that the ideal pulse has to be determined in a semi-anechoic chamber. This method also requires a large number of signals to create the ideal pulse for each device to be detected.

**3.1.2.3 Hurst parameter method.** Hurst Parameter is a measure for the long range dependence of a signal. A time series is considered to have long range dependence if there is a correlation between time series that sustains throughout the time scales [48]. A series is considered to possess long range dependence if the value

of Hurst parameter is between 0.5 and 1 [48]. Hurst Parameter was first used for UEE detection by Hertenstein et al. (2011). [49] used Hurst value is used as a threshold for differentiating noise and UEEs [49]. All the test signals with Hurst value above the threshold value is assumed to be UEEs. This method is based on the assumption that the long-range dependence characterized by the the Hurst parameter can be used as an indicator of presence of patterns of data. The experimental study found that ROC curve of the Hurst parameter was higher than the other methods [49].

The drawback of this method was that the range of detection was only 25cm and this method is not capable of differentiating between two or more devices. The false positive rate of this method, which is the detection of noise as an UEE, is so high that its practicality is limited. The minimum Hurst parameter for noise is calculated and any signals with higher hurst parameter is considered as UEE signals [39]. Higher false positive rate and the inability to differentiate between two or more devices are the drawbacks of this methods. Hurst parameters are difficult to measure [50], and this difficulty in measurement adds another limitation on this method.

**3.1.2.4 Granulometric size distribution.** The methods discussed so far for UEE detection is a threshold based method. In threshold based method, a specific threshold value is determined based on device characterization. Any value such as correlation coefficient or match filter value above the threshold value signifies a presence of device and value less than threshold signifies noise. Granulometric Size Distribution (GSD) method, proposed in [51], can be considered a novel method as it is not a threshold based method. The GSD of a given curve is a function of the structuring element size which plots the area under the opened curve against the area under the original curve [52]. GSD is basically a morphology based technique where a signal is characterized based on the shape of the curve. Any difference between the UEE signal and noise signal will be characterized in their GSD. That is, the GSD plot of UEE signal ideally should be different from the GSD plot of noise. This difference in shape of the signal can be used to differentiate between UEE and noise [51]. The next step is to classify the GSD curve of UEE from the GSD curve of

noise. Guardiola and Mallor (2013) accomplished this step by classifying the GSD curves from both the UEEs and the noise into two groups using the Partition Around Medoids (PAM) algorithm. PAM is a clustering algorithm that classifies data points based on the distances they are apart from each other and the cluster head called medoids represents the center of the classified class [53]. PAM has an advantage over k-means as the cluster head of k-means is just the means of the all the data points in that cluster whereas in the case of PAM the cluster head is one of the actual data points that is centrally located in that particular cluster [54]. This method works well in accurately detecting the UEEs but according to the results presented in [51] the false positive rate was considerably higher at 36 percent.

## 3.2. RECOGNITION METHODS

Recognition, for the purpose of this research, is defined as the process of identifying between two or more sources of UEEs. In case where there is an existence of two or more sources of UEEs, the process of recognition identifies and recognizes the individual source of UEEs. Recognition is a more sensitive process than detection because when multiple sources of UEEs exists, the process of detection can only determine that UEEs exists in that frequency band but cannot determine if there are UEEs from multiple sources. The process of recognition, however, can distinguish between multiple sources of UEEs.

**3.2.1 Neural Networks.** Neural Networks (NNs) are machine learning algorithms that are based on the functioning of human brain. A detailed discussion of NNs can be found in Section 4.4. NNs are used to detect and identify devices ranging from a toy truck to vehicles in [38] and [55]. The NNs presented in Dong et al. (2006) consists of a multilayer perceptron with 5 neurons and sigmoid activation function for the first hidden layer and 1 neuron and linear transfer function for the output layer [55]. The network was trained using the Levenberg-Marquardt algorithm. The amplitude vs time plot from eight frequency bands were selected as an input to the NN. This method yielded a good detection accuracy of 98 percent.

Dong et al. (2006) not only detected but also identified between Toyota Tundra, a GM Cadillac, a Ford Windstar, and ambient noise with 99 percent accuracy. Their NN architecture comprised of feedforward neural network trained with back propagation algorithm. The input features are the maximum spectral magnitude, average magnitude over a frequency band divided by the average magnitude over the entire time-frequency plot, standard deviation of magnitude over a frequency band, number of points within 3 dB of the maximum spectral magnitude and the number of pulses over a frequency band.

The major drawback of this method is that it is a black box model which doesn't give information regarding the actual procedure of generation and emissions of UEEs. The computational costs of NNs are generally higher as the training consists of many trials and errors to find the appropriate NN architecture parameter that gives the best result.

### 3.3. SUMMARY

The stimulated detection method requires detailed information about the electronic device and its emissions to create the external stimulation signal. In addition, extra devices are required for the purpose of generating the stimulus signal and then collecting the reflected stimulated UEEs. For example, the long PN code method discussed in Section 3.1.1.2 used USRP for the transmission and the receipt of the stimulus signal. Passive detection methods are the ones that doesn't require the stimulation signal.

The methods for UEE detection and recognition discussed in this section (except GSD and NNs) are threshold based methods. In threshold based methods, there is a need to quantify a certain threshold such that the decision can be made that detection occurs above the threshold. There are two disadvantages of threshold based methods: The first disadvantage is that the threshold value is calculated in a noise free environment of a semi-anechoic chamber, requiring extra work. The second disadvantage is that the threshold based methods can only be used for device detection but not for recognition. The reason for this limitation in threshold based

methods is that detection occurs for all the values higher than the threshold value. Any test value higher than the threshold value denotes a presence of device. But there is no way of identifying two or more devices.

The review of available literature in UEE detection methods demonstrates a lack of methods that are capable of not only detecting if there is a presence of device but also distinguishing between two or more devices. The capability of recognition of UEE makes the implementation of IED detection system for military operation more effective. For example, in a military field operation, some of the devices of the military may emit UEEs. In such circumstances, if the UEE detection system doesn't have the capability of differentiating between two or more devices, then the false alarm rate will be high. This research attempts to fill the gap by exploring stochastic and computational intelligence methods that can perform passive detection and recognition of malicious devices based on their UEEs. These methods will increase the effectiveness of the IED detection system by enhancing its detection and recognition capability with the less costly passive detection approach. The Neural Network method, described in section 3.2.1 is the only method that can not only detect devices, but can also identify and differentiate between devices. Two or more than two devices can be modeled by NNs by assigning different target values to each devices. Based on training data, NN will train itself to identify given targets as different devices. Even though NNs has the additional capability of identifying devices, there are some limitation. The selection of hidden nodes and training parameters is heuristic, all the parameters have to be re-estimated if one or more devices are added to the model. The computational cost of this method is high as training neural networks with large data set takes a significant amount of time.

The next section will discuss in details how Principal Components Analysis (PCA), Hidden Markov Model (HMM), and Support Vector Machine can be used in detecting and recognizing electronic devices based on their UEEs. As NN is the only method found in the literature that can not only detect but also identify different sources of UEE, this research will compare all the proposed methods of UEE detection and recognition with NNs for the purpose of validation.

## 4. METHODOLOGY

Section 3 reviewed the available literature on the detection of UEEs. There are many methods available that can detect the presence of UEE. But as discussed in the previous Section, most of those methods were threshold based methods. Being threshold based methods, they do not have the capability of differentiating between two or more sources of UEEs. This Section will explore the models that are capable of both detecting and recognizing UEEs. As the focus of this research is on the passive detection approach where the signals to be detected are weak in power and are often buried in the noise band, the methods should be versatile enough to overcome these challenges. This section investigates the performance of three methods, namely, Principal Components Analysis (PCA), Hidden Markov Models (HMMs), and Support Vector Machines (SVMs) that has the promise to meet the objective of recognition capability and overcome the challenge of low power signal buried in the noise band. This section will introduce the mathematical formulations of each of these methods and will discuss how these methods can be applied in detecting and identifying UEEs from RF devices. The common passive detection methods for UEE detection are discussed in sections 2.2.1 through 2.2.5. Specifically, the passive detection methods Matched Filter, Cascading Correlation, Hurst Parameter, and Granulometric Size Distribution have been applied to accurately detect the presence of UEEs. These methods can not, however, identify and differentiate between two sources of UEEs. There exists minimal difference between the properties of UEEs of two RF devices and thus the methods discussed in Section 3.1.2, with the exclusion of Neural Networks (NNs), are not sensitive enough to capture the differences. This work is not only about exploring new methods for accurately detecting UEEs, but it is also about finding new methods that can identify and recognize between two sources of UEEs. There is a need for more methods like Neural Networks that can

detect and identify two different but similar sources of UEEs.

#### 4.1. PRINCIPAL COMPONENTS ANALYSIS

Data that describe a process or a system are generally multivariate in nature [56]. As the dimension of data increases, so does the difficulty of analyzing and extracting useful information from such data. Data with large number of variables results in the curse of dimensionality, which is the exponential increase in data space that is required to train and gather information from such data set [57]. Silverman (1986) illustrates the problem of curse of dimensionality with the help of an example. He calculated the number of observations required to estimate the standard multivariate normal density function such that the Mean Square Error (MSE) is less than 0.1 [58]. The result of Silverman (1986) is illustrated in Figure 4.1.

It can be seen in Figure 4.1 that for a dataset of one dimension, four samples are enough to estimate the standard normal density function with MSE less than

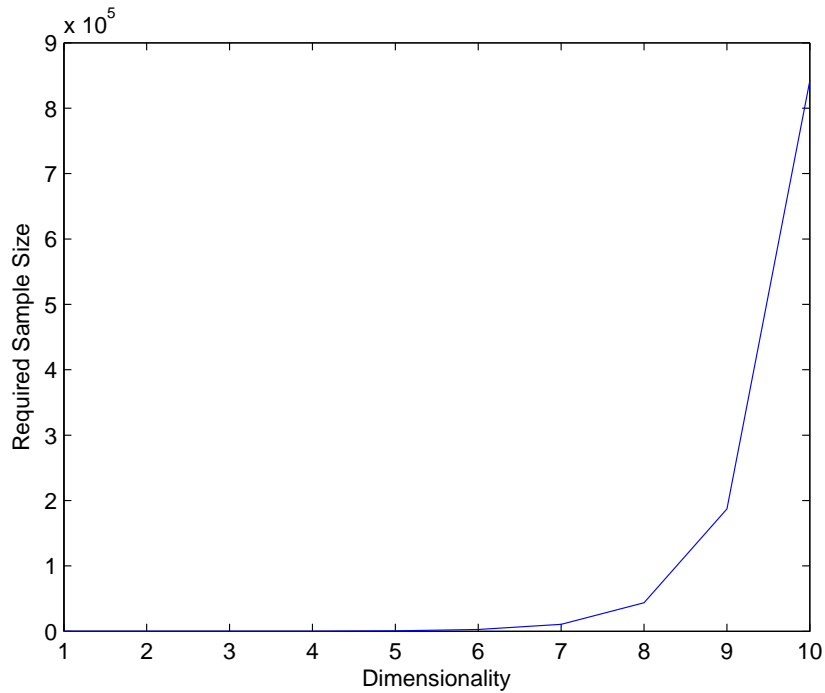


Figure 4.1 Number of Observations Required to Estimate the Standard Multivariate Normal Density Function such that the Mean Square Error is less than 0.1

0.1. But as the dimension of dataset increases, the required sample size to estimate the standard multivariate normal density increases tremendously to attain MSE less than 0.1. The figure shows that the required number of samples required to maintain the MSE error less than 0.1 requires 19, 223, 2790, 43700, and 84200 as the dimension of dataset increases to 2, 4, 6, 8, and 10 respectively. This increase in the required sample size with the increase in dimensionality of the dataset is commonly referred to as the curse of dimensionality.

One way to deal with the problem of curse of dimensionality is to reduce the dimension of the dataset. Principal Components Analysis (PCA) is one of the most common method used for reducing the dimensionality of data [59]. PCA reduces the original set of variables, into a new set of variables called principal components (PCs). PCs are the linear combination of original variables. The first PC is the direction that signifies the maximum variation in the original data set. The second PC is the direction that signifies maximum variation that is uncorrelated to the first PC. Similarly, subsequent PCs signify the directions of maximum variation that are uncorrelated to the previous PCs [60]. Moreover, as explained in 4.1.1, PCs are the Eigenvectors of the covariance matrix of the variables arranged by Eigenvalues [61]. The reduction in variable occurs as the transformation takes place from original set of variables to the PCs and the number of PCs are always less than or equal to the number of original variables. The original variables are represented by lesser number of PCs, thus reducing the dimensionality.

The concept of Signal to Noise Ratio (SNR) can be used to explain why PCA can be used for UEE detection. SNR is defined as the ratio of signal power to the noise power [44]. Shlens (2005) has demonstrated that the ratio of consecutive PCs is nothing but the SNR of the signal [62]. The ratio of two consecutive PCs of the noise signal has to be lower than the ratio of two consecutive PCs of the UEEs as the noise has lower SNR than the UEEs. Thus, fewer PCs will be able to explain most of the variation in UEEs whereas many PCs of noise signal will be required to explain most of its variation.

This concept can be verified with the help of examples. PCA was first performed

on White Gaussian Noise (WGN) to study the characteristics of PCs on WGN. Figure 4.2 demonstrates the contribution of top 10 PCs on those noise signals. It can be observed in Figure 4.2 that the top 10 PCA explains almost equal amount of variation in the data. The contribution of each of the top 10 PCs are about 3.5% and the top 10 PCs explain only about 32% of the variation in the dataset.

The PCA was then performed on the square signal, triangle signal, and the sawtooth signal with the same dimension as the noise signal. The pareto diagram of the top PCs of square, triangle, and sawtooth signals are illustrated in the Figures 4.3, 4.4, and 4.5. It can be observed in the figures that top 9 PCs explained 100% of the variation for all the three types of signals. But in the case of noise, the percentage of variation explained by top 10 PCs is only 32.29%. The contribution of top 10 PCs of the three signals and the noise is illustrated in Table 4.1 and Figure 4.6 for clarity. Noise are signals that fluctuates randomly. The variation of amplitude of noise signal is constant throughout the signal. Due to this constant variation in noise, all the PCs explains almost equal amount of variation. In case of any other signals, however,

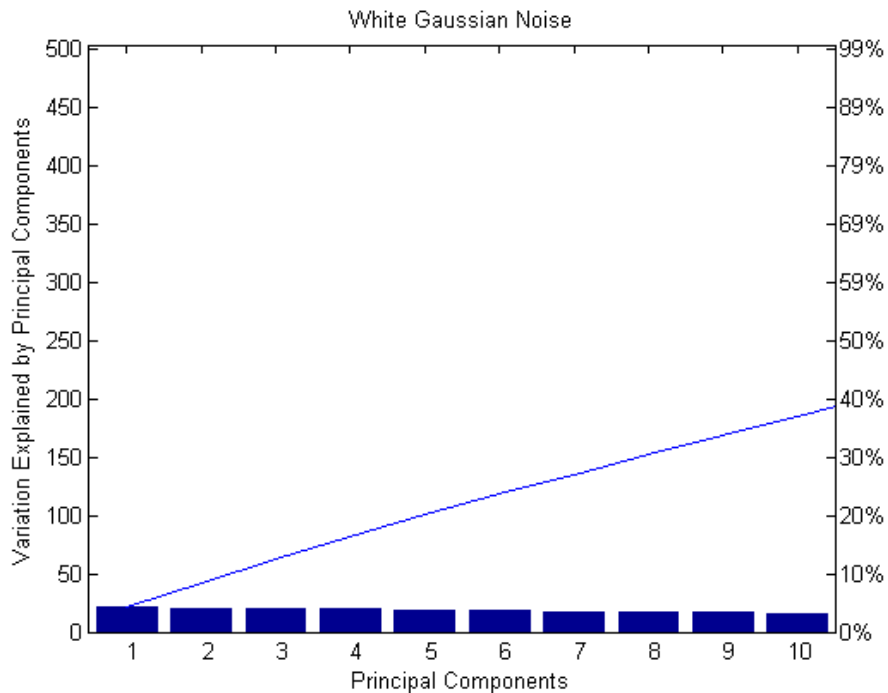


Figure 4.2 PCA of White Gaussian Noise

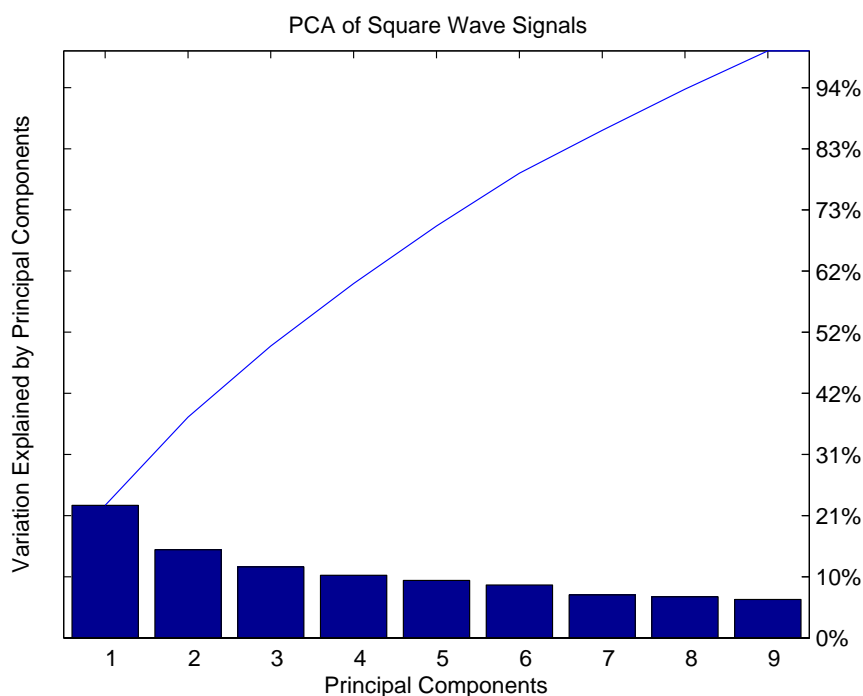


Figure 4.3 PCA of Square Signals

there is a variation of amplitude throughout the signal. The amplitude of the signal will be higher in some portion of the signal whereas it will be lower in other portions. Due to this variation of amplitude, the top PCs will explain most of the variation of the signal. Since the variation of amplitude of UEEs is not random, the top PCs of UEE will explain most of the variation. This property of PCA can be used to detect UEEs from noise.

PC	Square Signal	Triangle Signal	Sawtooth Signal	Noise
1st	22.59%	18.19%	16.44%	3.57%
2nd	37.60%	32.68%	31.57%	6.99%
3rd	49.70%	46.58%	44.97%	10.37%
4th	60.36%	58.96%	56.39%	13.63%
5th	70.16%	68.97%	67.34%	16.88%
6th	79.15%	78.09%	76.84%	20.04%
7th	86.46%	86.12%	85.47%	23.17%
8th	93.46%	93.54%	93.04%	26.24%
9th	100.00%	100.00%	100.00%	29.29%
10th	100.00%	100.00%	100.00%	32.29%

Table 4.1 Distribution of Variation Explained by Principal Components

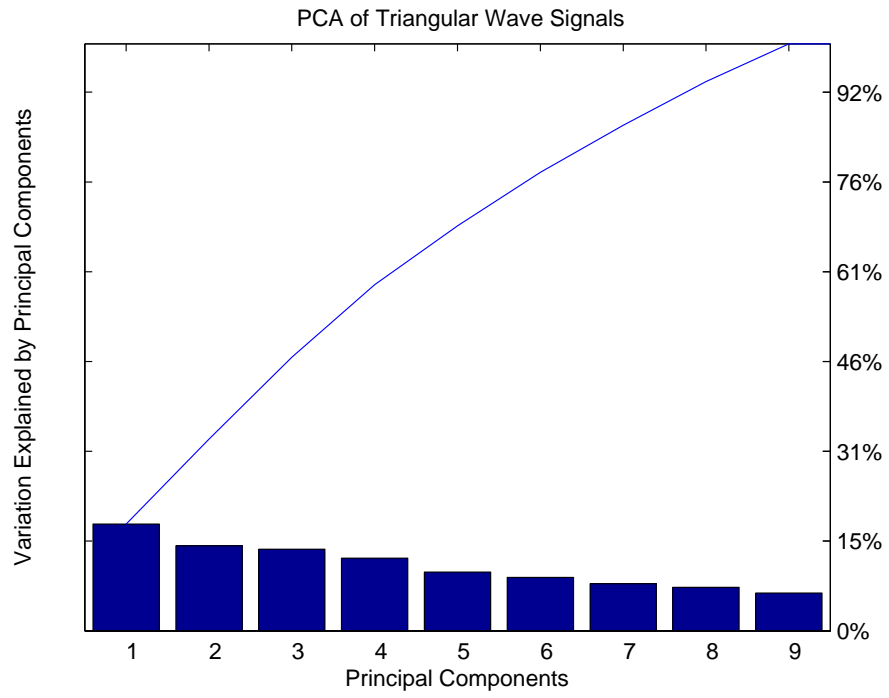


Figure 4.4 PCA of Triangle Signals

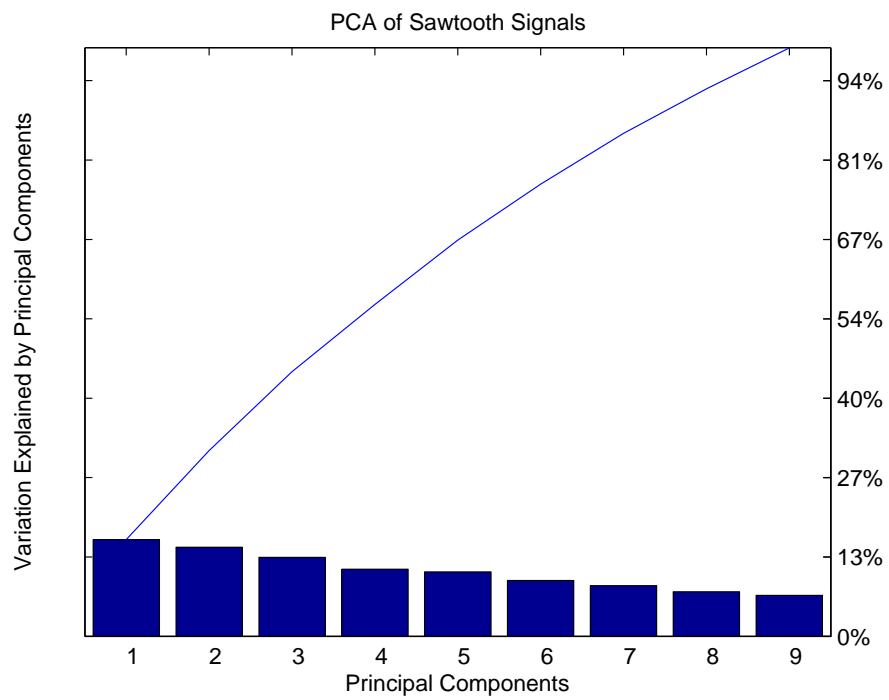


Figure 4.5 PCA of Sawtooth Signals

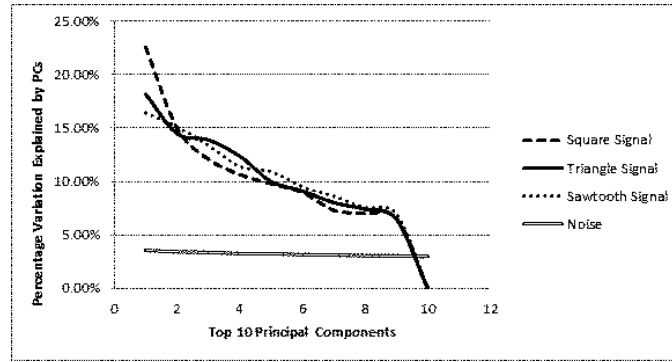


Figure 4.6 Percentage of Variation Explained by Each of the Top 10 PCs of Noise, Square Signal, Triangle Signal, and Sawtooth Signal

Section 4.1.1 will mathematically define the PCA approach and section 4.1.2 will discuss the PCA methodology employed with the UEE and noise dataset.

**4.1.1 Definition.** PCA is an eigenvalue analysis of the covariance matrix that ranks the components that explain most variation in the data [63]. The derivation of PCA given in [64] will now be briefly summarized.

Let  $A_p$  be input data where  $X$  is a set of  $m$ -dimensional input vectors with  $\{x_1, x_2, \dots, x_m\}$  as the  $m$  attributes. The objective of PCA is to find  $m$  dimensional orthogonal vectors  $l$  that can represent the variation in  $X$  such that  $l \leq m$  and  $l$  is the number of principal components. An orthogonal transformation matrix  $Q$  has to be found that can transform the original input vector  $X$  into a reduced dimensionality input vector  $X_r$  such that:

$$X_r = QX$$

Let  $a = [a_1, a_2, \dots, a_m]^T$  be a set of projections where  $\{a_j \mid j = 1, 2, \dots, m\}$ . The projection can now be defined as the inner product of the vector  $X$  and unit vector  $q$  such that

$$A_p = X^T q = q^T X$$

Let us denote the variation of  $A_p$  by  $\sigma^2$ , such that:

$$\sigma^2 = E[A_p^2]$$

$$\begin{aligned}
&= E[(X^T q)(q^T X)] \\
&= q^T E[XX^T]q \\
&= q^T Rq
\end{aligned}$$

where  $R$  is the correlation matrix of  $X$

Let  $a$  and  $b$  to be any  $m \times 1$  vectors, then

$$a^T Rb = b^T Ra$$

The variance of projection  $A_p$  can be written as a function of the unit vector  $q$  as follows:

$$\psi(q) = q^T Rq$$

The next step is to solve the following eigenvalue problem

$$Rq = \lambda_p q \tag{1}$$

where  $\lambda_p$  are the eigenvalues of the correlation matrix  $R$  and the values of  $q$  associated with  $\lambda_p$  are the eigenvectors.

Eigenvalues  $\lambda_p$  is computed using the relation

$$(R - \lambda_p I)q = 0$$

The eigenvectors  $Q = [q_1, q_2, \dots, q_m]$  represent the set of orthogonal vectors of the projection and the associated eigenvalues define the contribution of each eigenvector to the overall variation in the data. Total variance of the projected data is given by  $\sum_{j=1}^l (\lambda_p)_j$

The percentage of variation of individual component denoted by  $P_r$  is given by:

$$P_r = \frac{(\lambda_p)_l}{\sum_{j=1}^l (\lambda_p)_j} \tag{2}$$

$$Power(Watt) = 10^{[(Power(dBm)-30)/10]} \tag{3}$$

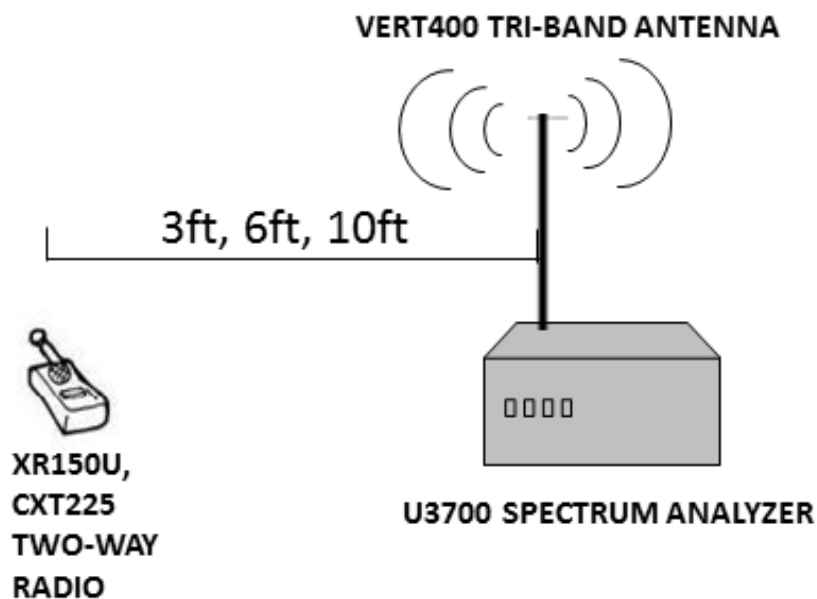


Figure 4.7 Experimental Setup for Data Collection

Orthogonality of the transferred variables is one of the important assumption of PCA [65]. Principal Components, the transferred variable in PCA are the variables that should be orthogonal to each other. Principal Components are the eigenvectors of the covariance matrix, and since eigenvectors are orthogonal to each other, the assumption of orthogonality of the transferred variables are satisfied.

**4.1.2 UEE Detection Using PCA.** Data collection for this project was done using U3700 spectrum analyzer by Advantest and VERT400 tri-band antenna. CXT225 Two-Way Radio from Cobra MicroTalk and XR150U Business Two-Way Radio are selected as simple RF radios for the purpose of proof of concept exploration. The reference name of D1 and D2 will refer to the previously mentioned RF receivers respectively. The operating frequency of the devices is from 450 to 470 MHz. As UEEs have very low power emissions, for the purpose of clarity, a 20 KHz span was chosen for each device. The span of D1 was from 441001.140 kHz to 441021.140 kHz and the span of D2 was from 438215.064 kHz to 438235.064 kHz. The readings were taken at 3, 6, and 10 feet from the spectrum analyzer. So there are data sets for seven cases with six cases for two devices at three different distances and one case

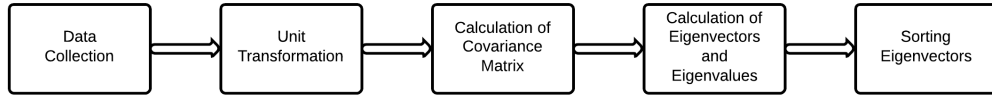


Figure 4.8 Application of PCA for UEE detection

for noise collected within the same operating environment. A schematic setup for data collection is shown in Figure 4.7. To collect data, the spectrum analyzer was set to -30db level to appropriately display the signal on screen. On every collection instance of an UEE, a sample of 1,001 points are stored. 40 such instances of UEE are collected for noise and both D1 and D2 at three distances.

**4.1.3 Feature Extraction.** The process flow diagram for UEE detection is illustrated in Figure 4.8. The first step is collecting the data. A detailed explanation of how the data was collected for two devices for three different distances and for noise is explained in section 4.1.2. The second step is the data preparation step. The unit of dBm is a logarithmic scale, so it is converted to Watt for easier calculation using Equation 3. All the data computations are done by computer software and they utilize their own built-in algorithms for calculating data. But even the basic operation like multiplication is different for a log data than for any other type of numeric data. The conversion from decibel to watt ensures that the data processing software doesn't take decibel data like any other numeric data and perform mathematical operations that results in unwanted results. A covariance matrix is then calculated for each dataset. If there are  $m$  observations of amplitude against frequency, then the dimension of covariance matrix  $R$  will be  $m \times m$ . Since there are 1001 observations of amplitude against frequency, the dimension of the covariance matrix is  $1001 \times 1001$ . As all covariance matrix are square matrix, eigenvectors and eigenvalues is calculated for the covariance matrix  $R$  by solving the Equation 1. The eigenvectors are then ordered based on the value of their eigenvalues. The percentage contribution of each component was calculated by dividing the percentage component of each PC by the

sum of all percentage contribution using Equation 2. The results are discussed in Section 5.1.

## 4.2. HIDDEN MARKOV MODELS

Hidden Markov Models (HMMs) are doubly embedded stochastic process in which one stochastic process is a markov chain that is not observable and another is an observable stochastic process. Inference about the hidden process is made through its relationship with the observable process. Figure 4.9 illustrates the basic structure of an HMM. The hidden layer consist of a Markov chain in which the states are denoted by  $S_1, S_2, \dots, S_n$ . The Markov chain cannot be observed directly because it is a hidden layer. There is another stochastic process which is observable and is related to the hidden Markov chain. The observations of this stochastic process are denoted by  $O_1, O_2, \dots, O_n$  in Figure 4.9. Inference about the hidden layer, and thus the system in general is made by a set of well developed algorithms such as forward algorithm, Viterbi algorithm, and Baum-Welch algorithm. Details of these algorithms are discussed in Sections 4.2.3, 4.2.4, and 4.2.5.

HMMs are used in a number of areas. They are particularly useful in stochastic processes in which complete information on the transition of a system from one state to another is unavailable, but there exists another stochastic process which is observable and is dependent on the hidden process. HMMs have been successfully used in speech recognition [66], biological sequence recognition such as protein sequence recognition and DNA sequence recognition [67], gesture recognition [68], handwriting recognition [69], and more. Some researchers have even attempted to apply HMM to detect rare events like earthquake [70].

Gesture recognition system can be modeled using HMM by representing the silhouettes of gait cycle as observations and the different boundaries formed by the pixels of the silhouette plots as the hidden states [71]. HMM can model facial expression detection by representing different features from the face videos as observations and the flow of different emotions of human beings as hidden states [72]. HMM can

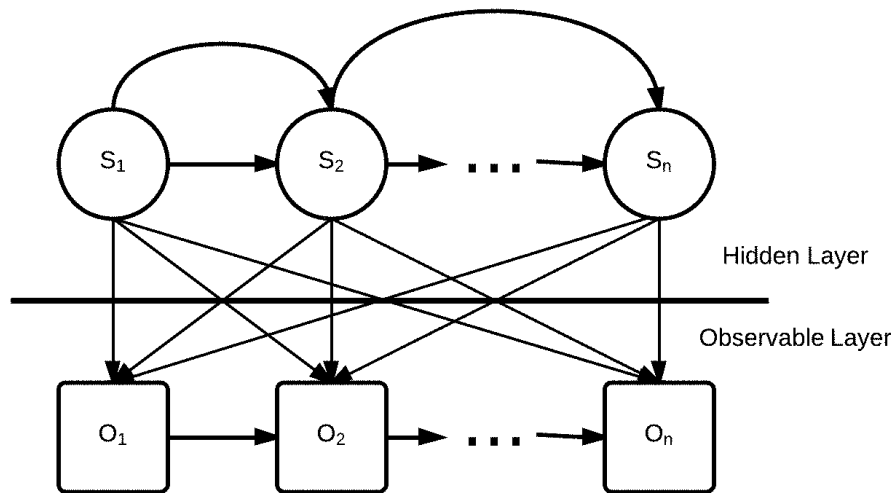


Figure 4.9 Basic Structure of Hidden Markov Model

be used to label any unlabeled string of nucleotides by representing the nucleotide sequence as observations and different DNA sequence as the hidden states [73]. In case of handwriting recognition system, features extracted from writing like the angle between two successive points measured at regular intervals can be considered as observations and combinations of characters can be considered as hidden states [69]. In speech recognition, perhaps the most successful application of HMM, acoustic feature vectors such as mel-frequency cepstrum coefficients are used as states and the different phonemes of sound are used as observations [74]. In case of earthquake detection, Beyreuther et. al (2012) modeled HMM by using the principal components of seismogram data as observations and the clustered data of different geological events as hidden states [75]. The next section discusses the observations and hidden states of HMM as it relates to UEEs.

**4.2.1 HMMs and UEEs.** It has been illustrated in Figure 2.4 and Figure 2.5 that UEEs are generated due to the leakage in internal circuitry of the device. The leakages then couple with the device's antennae and is emitted to the outside environment as UEEs. Since it is extremely difficult to predict the actual amount of

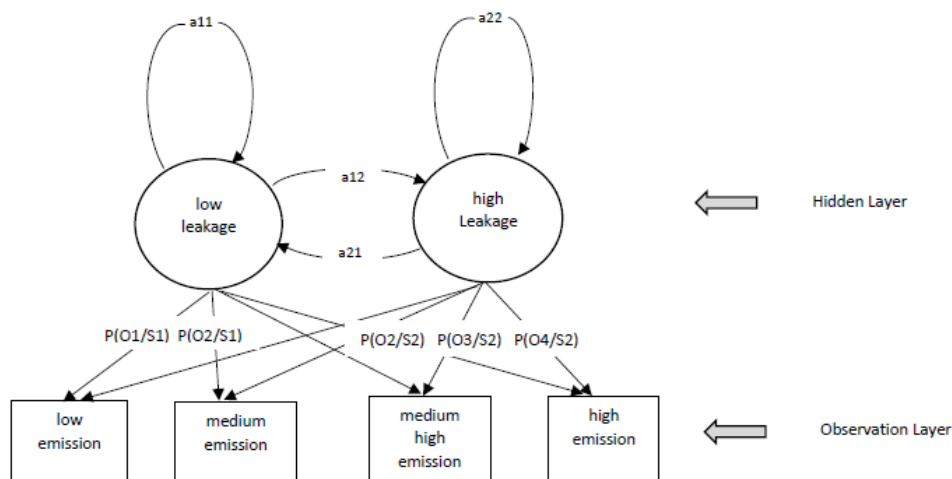


Figure 4.10 Hidden Markov Model for UEE Identification

leakage at a point in time, we cannot accurately model the UEE generation process directly. But the properties of UEEs after they are generated and unintentionally emitted to the outside environment can be measured. This process can be modeled using HMM: The information gathered from the observation can be used to infer the inside working mechanisms of the device that produced the UEEs. This process is schematically described in Figure 4.10. The leakage from electromagnetic devices are classified into two types: lower power leakage and higher power leakage. These two leakages are taken as the two hidden states and are referred as low leakage and high leakage. Low leakage is taken as state 1 and high leakage is taken as state 2. It is very difficult to measure the total leakage from the device, but the unintended emissions due to the leakages from various sources of the internal circuitry can be measured. These measurable observations are classified into four classes: low emission, medium emission, medium-high emission and high emission. HMMs with unique parameters for each devices can be constructed using the information of hidden state and observations. The overall signal identification process is illustrated in Figure 4.11.

**4.2.2 Definition.** Hidden Markov Models (HMMs) are doubly embedded stochastic process with an underlying stochastic process that is not observable, but can only

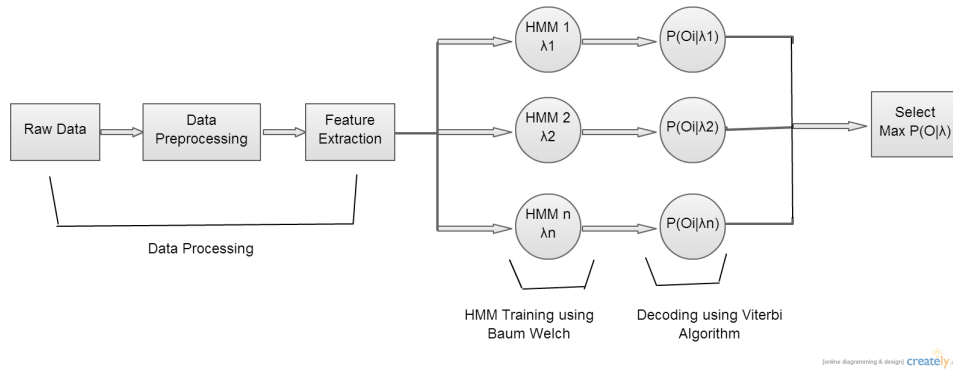


Figure 4.11 Signal Identification Process

be observed through another set of stochastic processes that produce the sequence of observations [66]. We can define an HMM by the following five elements [66].

1. The number of states in the model is the first element to define an HMM. We will denote this number by  $N$ . It represents the total number of states present in the hidden stochastic process. The individual states will be denoted as  $S = \{S_1, S_2, \dots, S_N\}$ .
  2. The second element to characterize the HMM is the number of observation symbols. It represents the total number of distinct observations and we represent it by  $T$  in this paper. The individual observations will be represented by  $O = \{O_1, O_2, \dots, O_T\}$ .
  3. The state transition probability distribution is the third element of HMM. We represent it by  $A = \{a_{ij}\}$  where  $a_{ij} = P[q_{t+1} = S_j \mid q_t = S_i]$ ,  $1 \leq i, j \leq N$
  4. The observation symbol probability distribution in state  $j$ ,  $B = \{b_j(k)\}$  where  $b_j(k) = P[O_k = t \mid q_t = S_j]$ ,  $1 \leq j \leq N$ ,  $1 \leq k \leq M$
  5. The initial probability distribution is the fifth element that characterize HMM and it is represented by  $\pi = \{\pi_i\}$  where  $\pi_i = P[q_1 = S_i]$ ,  $1 \leq i \leq N$
- for convenience, an HMM is denoted by the tuple  $\lambda = (A, B, \pi)$

**4.2.3 Three Problems for HMM.** There are three problems that can be solved by a HMM [66]. They are:

1. The evaluation problem is the computation of the probability that a given set of observations is produced by a particular HMM. This makes it possible to choose a best model from a set of competing models. Mathematically, if a set of observation is represented by  $O = \{O_1, O_2, \dots, O_T\}$  and we have a HMM  $\lambda = (A, B, \pi)$ , evaluation problem is the calculation of  $P(O | \lambda)$ . This is solved using the forward algorithm.
2. The decoding problem is concerned with the calculation of most likely states that generate a given set of observations. This problem is essentially to decode the hidden state from visible set of observations. Mathematically, given  $O = \{O_1, O_2, \dots, O_T\}$  and  $\lambda = (A, B, \pi)$ , the decoding problem is to calculate the most likely sequence of states the hidden stochastic process went through to generate  $O$ . This problem is solved by the Viterbi algorithm.
3. The learning problem is related to the training of the model parameters. We want to train  $\lambda = (A, B, \pi)$  with the objective of maximizing  $P(O | \lambda)$ . This is solved using Baum Welch algorithm.

**4.2.4 Solution to the Evaluation Problem.** The problem in this case is to calculate  $P(O | \lambda)$ , which is to calculate the probability of occurrence of the observation sequence  $O = O_1, O_2, \dots, O_T$  given the model  $\lambda = (A, B, \pi)$ . To solve this problem, a forward variable  $\alpha_t(i)$  is defined such that:

$$\alpha_t(i) = P(O_1, O_2, \dots, O_t, q_t = i | \lambda)$$

Forward probability is defined as the probability of the partial observation sequence  $O_1, O_2, \dots, O_t$  and state  $i$  at time  $t$ , given the model  $\lambda$  [66].  $\alpha_t(i)$  can be solved inductively as follows:

1. The first step initializes the forward probabilities as the joint probability of state  $i$  and initial observation  $o_1$  as follows:

$$\alpha_1(i) = \pi_i b_i(o_1), 1 \leq i \leq N$$

2. The second step is of induction which shows how state  $j$  can be reached at time  $t+1$  from the  $N$  possible states at time  $t$ :

$$\alpha_{t+1}(j) = \{\sum_{i=1}^N \alpha_t(i) a_{ij}\} b_j(o_{t+1}), 1 \leq t \leq T \text{ and } 1 \leq j \leq N$$

3. The third step gives the value of  $P(O | \lambda)$  by summing all the forward variables  $\alpha_T(i)$  :

$$P(O | \lambda) = \sum_{i=1}^N \alpha_T(i)$$

**4.2.5 Solution to the Decoding Problem.**  $\delta_t(i)$  is defined as the best score along a single path, at time  $t$ , which accounts for the first  $t$  observations and ends in state  $i$  as:

$$\delta_t(i) = \max_{q_1, q_2, \dots, q_{t-1}} P[q_1, q_2, \dots, q_{t-1}, q_t = i, o_1 o_2 \dots o_t | \lambda]$$

By induction,

$$\delta_{t+1}(j) = [\max_i \delta_t(i) a_{ij}] \cdot b_j(o_{t+1})$$

Another variable  $\psi_1(i)$  is defined to keep track of the argument that maximized  $\delta_{t+1}(j)$  for each value of  $t$  and  $j$ . Following steps summarize the viterbi algorithm:

1. First step initializes the variables  $\delta_t(i)$  and  $\psi_1(i)$  such that

$$\begin{aligned} \delta_t(i) &= \pi_i b_i(o_1), 1 \leq i \leq N \\ \psi_1(i) &= 0 \end{aligned}$$

2. Subsequent values for the variables initialized in step 1 is calculated by the process of recursion

$$\begin{aligned} \delta_t(j) &= \max_{1 \leq i \leq N} [\delta_{t-1}(i) a_{ij}] b_j(o_t), 2 \leq t \leq T \text{ and } 1 \leq j \leq N \\ \psi_1(i) &= \arg \max_{1 \leq i \leq N} [\delta_{t-1}(i) a_{ij}], 2 \leq t \leq T \text{ and } 1 \leq j \leq N \end{aligned}$$

3. Third step is to terminate the recursion started in step 2

$$\begin{aligned} P^* &= \max_{1 \leq i \leq N} [\delta_T(i)] \\ q_T^* &= \arg \max_{1 \leq i \leq N} [\delta_T(i)] \end{aligned}$$

4. The final step consists of determining the state sequence by backtracking the variable  $\psi_1(i)$  defined earlier

$$q_t^* = \psi_{t+1}^*(q_{t+1}^*), t = T-1, T-2, \dots, 1$$

**4.2.6 Solution to the Learning Problem.** In HMM, the term learning denotes the process of training the algorithm based on existing data set [66]. To solve the learning problem, a variable  $\xi_t(i,j)$  and  $\gamma_t(i)$  is defined such that

$$\begin{aligned}\xi_t(i,j) &= P(q_t = i, q_{t+1} = j \mid O, \lambda) \\ \gamma_t(i) &= P(q_t = i \mid O, \lambda)\end{aligned}$$

Following are the re-estimation formula for the HMM parameters:

$$\begin{aligned}\pi_i &= \gamma_o(i) \\ a_{i,j} &= \frac{\sum_{t=1}^T \xi_{t-1}(i,j)}{\sum_{t=1}^T \gamma_{t-1}(i)} \\ b_j(k) &= \frac{\sum_{t=1}^T \xi_{t-1}(i,k)}{\sum_{t=1}^T \gamma_{t-1}(i)}\end{aligned}$$

**4.2.7 Data Collection and Preprocessing.** The data collection process is described in Section 4.1.2. The raw data was converted from dBm to Watt using Equation 3. The reason for this conversion is that the dBm data is in logarithmic scale. All the data calculations are done by computer software and they utilize their own built in algorithms for calculating data. But even the basic operation like multiplication is different for a log data than for any other type of numeric data. The conversion from decibel to watt ensures that the computer doesn't take decibel data like any other numeric data and perform mathematical operations that results in unwanted results. Windowing operation was then performed on each instances of data. Each window consisted of 100 data points and has an overlap of 50 data points.

**4.2.8 Feature Extraction.** Some features from the observable process is required to model a system by HMM. The average power of the signal in each window created is taken as the feature vector of the UEE signal. The process of creation of window is described in 4.2.7. Average power is calculated by integrating the power at each frequency of the window by rectangular approximation and dividing by the number of samples in the window as shown in Equation 4.

$$\frac{1}{w_2 - w_1} \int_{w_1}^{w_2} S_x(w) dw \quad (4)$$

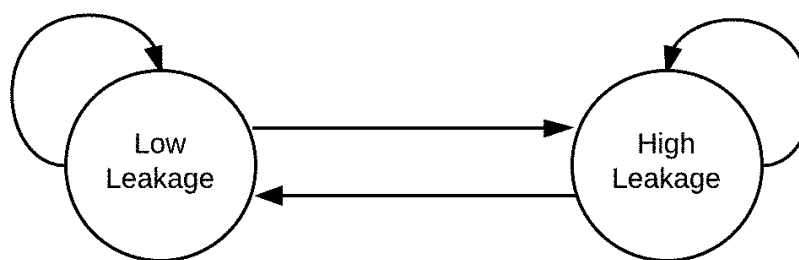


Figure 4.12 Ergodic Markov Chain

**4.2.9 Training.** The four levels of emissions are the four observations of the HMM and the two levels of overall device leakage are the two hidden states. The topology of Markov chain is ergodic for the UEE is taken as ergodic. Figure 4.12 illustrates the ergodic Markov chain for the UEE Markov chain. An ergodic Markov chain is one where it is possible for a state of the Markov chain to reach any other state. The leakage from the RF devices are taken as states. The two states are *low emission* and *high emission*. Since the states represents the leakage of the device, having just one state is not enough to capture the different levels of leakage from the device. But two states can model the leakage of device by allowing the device to be either in one of the low emission leakage state or high emission leakage state. Even though more number of states can be taken, two states can accurately model the differences in the leakage level from the device. As the state can move from low emission to both low emission and high emission and from high emission to both high emission and low emission, ergodic markov chain is the most natural topology to represent UEE emission. The average power are the observations and there are four discretized observations which are *low emission*, *medium emission*, *medium-high emission* and *high emission*. The observations are the set of features extracted from the UEE signal discussed. In the case of UEE signal, the observations are the average power. The calculation of the observed power for each window is discussed in Section 4.2.8. The average power is divided into four interquartile range and each range is taken as one of the four observation signal. These observations

are passed as an input to the Baum Welch algorithm to train the HMM discussed in Section 4.2.6. HMMs are trained with these observation with the 30 training data set. Maximum Iteration value of 500 or the tolerance of  $10^{-6}$ , whichever is first achieved is taken as the stopping criteria for the Baum Welch algorithm. The initial probability for each state is taken as 0.5. The output of this process is a trained HMM. Viterbi algorithm discussed in Section 4.2.5 was then applied to the trained HMM. A pairwise comparison of  $D1$  and  $D2$  at three different distances of 3 feet, 6 feet, and 10 feet was performed. Pairwise comparison of both devices at three distances was also performed with noise. The results of the experiment are illustrated on the Results section.

**4.2.10 Assumptions of HMM.** Statistical methods are based on some underlying assumptions. Like any other models the theory of HMMs are also based on some assumptions. According to Rabiner (1989), and Bhat et. al (2002), the Markovian assumption is the major assumption to the theory of HMM [66], [76]. The Markovian assumption states that the probability of being in a given state at time  $t+1$  is depended only on the state at time  $t$  and not on any previous states, such that:

$$a_{ij} = P[q_{t+1} = S_j \mid q_t = S_i], 1 \leq i, j \leq N$$

This assumption pose a serious limitations on the applicability of HMMs. Various applications of HMMs were discussed in Section 4.2. Speech recognition is considered to be the most successful application of HMMs [77]. One of the most cited paper on speech recognition system is by Rabiner (1989) but he unequivocally states in the paper that these assumptions are violated for speech sounds. One of the beauties of HMMs lies in the fact that in spite of the limitations of assumptions of HMMs being violated, the method works extremely well in speech recognition problem [66].

The Markovian assumption can be verified by testing for the null hypothesis of independent Markov chain against the alternate hypothesis of first order Markov chain:

Null Hypothesis ( $H_0$ ):  $a_{ij} = P[q_{t+1} \neq S_j \mid q_t = S_i], 1 \leq i, j \leq N$

Alternate Hypothesis ( $H_1$ ):  $a_{ij} = P[q_{t+1} = S_j \mid q_t = S_i], 1 \leq i, j \leq N$

The  $\chi^2$  test statistic to test independence against first order Markovian dependence is given in [78] as:

$$\chi^2 \text{ test statistic} = 2 \sum_{i=1}^n \sum_{j=1}^n f_{ij} \left| \ln \frac{P_{ij}}{P_{.j}} \right| \quad (5)$$

with  $(n - 1)^2$  degree of freedom, where,

$n$  = number of states

$f_{ij}$  = the frequency of state transitions from state  $i$  to state  $j$

$$P_{.j} = \frac{\sum_{i=1}^n f_{ij}}{\sum_{j=1}^n f_{ij}}$$

The data collected from two devices at three different distances were converted from dBm to Watt using Equation 3 in order to test the hypothesis. Windowing operation was then performed as discussed in Section 4.2.7 and average power for each window is calculated using Equation 3. The details of data processing steps can be found in Section 4.2.7 and Section 4.2.8. The value of  $n$  is taken as 2 as the HMM for UEE is modeled by two states.  $f_{ij}$  is calculated using TPM for Markov chain as calculated and explained in Section 4.2.9. The only difference between the TPM calculated in Section 4.2.9 and here is that in Section 4.2.9, only 30 data set were used to calculate TPM for the training purpose, but for the verification of Markov assumption, all 40 available data sets were used to calculate the TPM.

Device	Chi Square Value	p value	Verdict
Device 1 at 3 ft	325.7302	<0.00001	Reject $H_0$
Device 1 at 6 ft	541.5781	<0.00001	Reject $H_0$
Device 1 at 10 ft	559.5422	<0.00001	Reject $H_0$
Device 2 at 3 ft	278.7866	<0.00001	Reject $H_0$
Device 2 at 6 ft	312.0549	<0.00001	Reject $H_0$
Device 2 at 10 ft	528.0602	<0.00001	Reject $H_0$
Noise	565.5422	<0.00001	Reject $H_0$

Table 4.2 Chi Square Test for First Order Markov Chain

Table 4.2 summarizes the results of  $\chi^2$  test for first order Markov assumption. It can be observed in the Table that the calculated  $\chi^2$  value for all the seven cases is greater than the tabulated  $\chi^2_{(0.05,1)}$  value of 3.841. The null hypothesis of independent Markov chain is thus rejected and we assume that first order Markovian assumptions holds true.

### 4.3. SUPPORT VECTOR MACHINE

The mathematical theory of Support Vector Machine (SVM) was developed by Vapnik in the 90s [79], [80]. SVM is generally used for pattern classification and nonlinear regression [64]. In SVM, the margin of separation between different classes of input vectors is maximized by the separating hyperplane. An illustration of SVM is illustrated in Figure 4.13. The figure illustrates how two class of linearly separable vectors, which are represented by circles and squares, are separated by SVM. The vectors which are closest to the separating plane are called the support vector. It is denoted by *SV* in Figure 4.13. SVM considers only the support vectors while constructing the separating plane. There can be many plane that can separate the two class of vectors. For example, in Figure 4.13, *L1*, *L2*, and *L3* are the three separating plane that separates the vectors into two distinct classes. The separating plane created by the SVM is such that the margin of separation between the separating plane and the vectors is highest. It can be observed in Figure 4.13 that *L1* is the plane where the margin of separation is the highest.

SVM is mostly applied to the problems that are related to pattern classification and nonlinear regression [81].

A mathematical representation of SVM will now be presented. If  $(x_i, d_i)$ ,  $i = 1, \dots, N$  be a set of patterns where  $d_i \in \{+1, -1\}$  then the separating hyperplane created by SVM is represented by:

$$w^T x + b = 0, \text{ where } w \text{ and } b \text{ are the weight vectors and the bias.}$$

The input points closest to the separating hyperplane are called support vectors. In Figure 4.13, the support vectors are represented by *SV*. We can observe in Figure 4.13 that there are two support vector for square class and two support vector for class

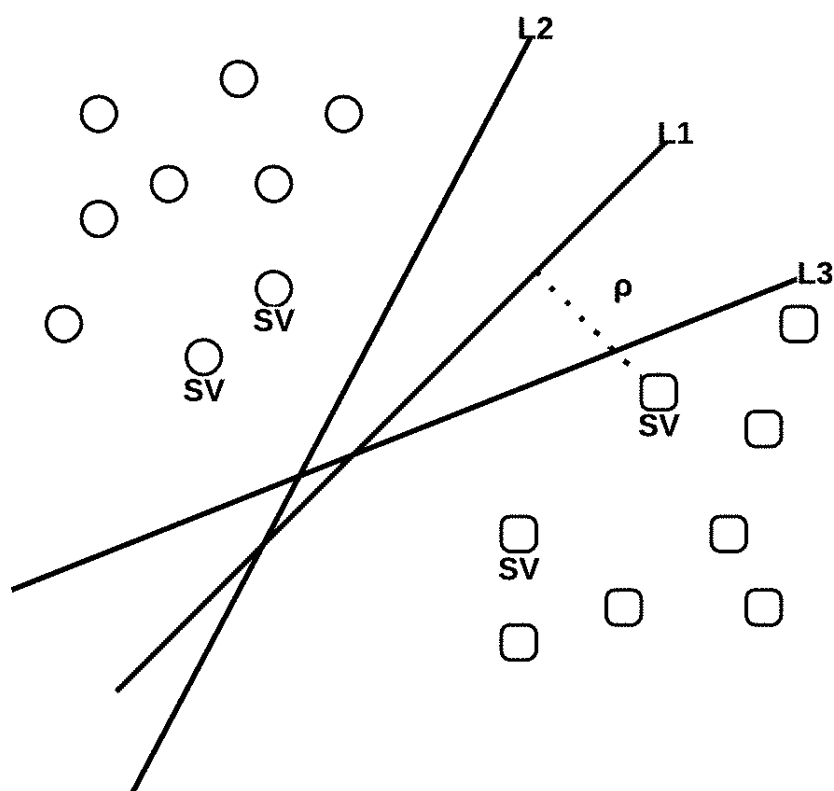


Figure 4.13 Support Vector Machine

the circle class. The margin of separation, denoted by  $\rho$ , is the distance between the separating hyperplane and the support vectors. Unlike other classifiers like Neural Networks, SVM creates the separating hyperplane that maximizes the margin of separation. So  $L1$  is the separating hyperplane created by SVM in Figure 4.13. Optimum values of the weight vector and bias, represented by  $w_0$  and  $b_0$  are given by:

$$w_0 = \sum_{i=1}^N a_{0,i} d_i x_i \text{ where } a \text{ is Lagrange multiplier}$$

$$b_0 = d^{(s)} - w_0^T x^{(s)}$$

Please refer to [64] for detailed derivation.

SVM are equally capable of separating non linear patterns. The two theorems that enables SVM in separating non linear data set are the Cover's Theorem and the Mercer's Theorem. Cover (1965) states that "A complex pattern-classification

problem, cast in a high-dimensional space nonlinearly, is more likely to be linearly separable than in a low-dimensional space, provided that the space is not densely populated” [82]. So a data set that is not linearly separable can be separated by projecting it into some higher dimensional space. There is no need to calculate the weight vector  $w_0$  and just specifying the kernel will perform the task of data separation in the higher dimensional space and this procedure is called kernel trick [64]. Mercer’s Theorem is applied to determine if a particular kernel function can be used in SVM. It states that the general form of inner product is defined by the function  $K(x, y)$  that satisfies the condition:

$$\int \int K(x, y)z(x)z(y)dx dy \geq 0$$

for all functions  $z(x)$ ,  $z(y)$  satisfying the inequality

$$\int z^2(x)dx \leq \infty \text{ [80].}$$

Radial basis function, which can be represented as:

$$K(x, x_i) = \exp \left\{ -\frac{|x-x_i|^2}{\sigma^2} \right\}$$

is one of the kernel that satisfies Mercer’s conditions [64].

30 data set was used for training purpose and 10 were used as testing purpose for two devices at three different distances. Support vector machine was run on R programming language, version 3.0.0 using e1071 package. Radial basis was the kernel used in training and predicting purpose because it satisfies Mercer’s conditions. The results of this experiment is illustrated in Section 5.

#### 4.4. NEURAL NETWORKS

Artificial Neural Networks (ANNs), commonly abbreviated as Neural Networks (NNs) are machine learning algorithms that is based on the functioning of human brain. Wernick et. al (2010) defined machine learning as a set of methods to make predictions on a new data set based on the relationship of variables that is learnt and understood in the existing data set [83]. This definition defines machine learning as a two step process. The first step consists of learning the relationship between variables in data set. The second step consists of making predictions based on the

knowledge gained in the first step on a new data set that is not part of the training process.

Neural Networks have been successfully used to solve many problems from different areas. Widrow et. al (1994) identifies three key areas of successful application of NNs and they are Pattern Recognition, Financial Analysis and Prediction, and Optimization and Control [84]. Credit card fraud detection is one of the most well known pattern recognition application of NNs. One of the earliest application of credit card fraud detection using Neural Networks was developed by Ghosh et. al (1994). They trained the NNs with different credit card transactions and used target values such as fraud transaction from lost card, stolen card, and counterfeit card. This NNs based credit card fraud detection system was implemented in Mellon Bank's credit card portfolio as the NNs were able to detect more fraudulent transactions with 20% less false positive prediction than the traditionally used rule based detection system [85].

Stock market price forecasting is another major application of NNs. The reason that NNs is an effective method for stock market forecasting is that financial market exhibit non linearity and NNs is a very good tool to model nonlinear process [86]. Hawley et. al (1990) were one of the earliest researchers proposing the application of NNs for financial decision making [87]. In one of the application of NNs in stock market price prediction, Schierholt et. al (1996) trained NNs with inputs such as closing value of current day's S & P 500 Index value, change in index value in one week and two weeks. The network was designed with three output: buy, sell, and keep current status. The result demonstrated that NNs gave better performance relative to the & P 500 Index [88].

NNs have been used to detect electronic devices through their UEEs. NNs are used to detect and identify devices ranging from a toy truck to vehicles in [38] and [55]. The NNs of Dong et al. (2006) consists of a multilayer perceptron with 5 neurons and sigmoid activation function for the first hidden layer and 1 neuron and linear transfer function for the output layer. The network was trained using the Levenberg-Marquardt algorithm. The amplitude vs time plot from eight frequency

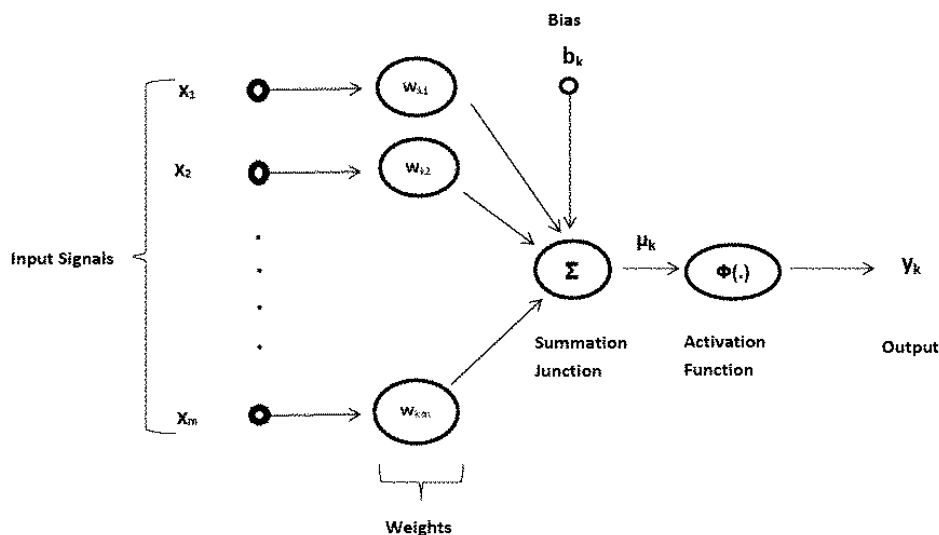


Figure 4.14 Neural Networks

bands were selected as an input to the NN. This method yielded a good detection accuracy of 98 percent.

Dong et al. (2006) not only detected but also identified between Toyota Tundra, a GM Cadillac, a Ford Windstar, and ambient noise with 99 percent accuracy. Their NN architecture comprised of feedforward neural network trained with back propagation algorithm. The input features are the maximum spectral magnitude, average magnitude over a frequency band divided by the average magnitude over the entire time-frequency plot, standard deviation of magnitude over a frequency band, number of points within 3 dB of the maximum spectral magnitude and the number of pulses over a frequency band. The accuracy of this method is 99.3%. As NNs have been successfully used to detect and identify devices using their UEEs, the performance of the proposed methods in this research would be compared to the performance of the NNs for the validation purpose.

Figure 4.14 shows a schematic diagram of a NN.  $x_1, x_2, \dots, x_m$  are the input signals to the NNs and  $w_{kj}$  where  $j$  is the input index and  $k$  is the neuron index.  $\mu_k$  is the output of the summation junction and the output signal  $y_k = \phi(\mu_k + b_k)$  where  $\phi$  is the activation function and  $b_k$  is the bias. The NN used backpropagation learning algorithm with Sigmoid activation function. There were two hidden layers and five

number of inputs. The learning rate was 0.5. The stopping criteria was maximum iteration of 1000 or minimum gradient of 0.0001, whichever was first reached. The results of this experiment is illustrated on Section 5.

This section provided the theoretical background on PCA, HMM, SVM, and NN. It also described the methodology on how these methods can be used to detect and recognize electronic devices based on their UEEs. Since NN is the only method found in the literature that can not only detect but also identify different sources of UEE, comparison of PCA, HMM, and SVM is done with NN. Next Section will provide the results of the performance of the three methods (PCA, HMM, and SVM) and its comparative performance as it relates to NN.

## 5. RESULTS

Three new methods are proposed in this research for passive detection of UEEs. The three methods are PCA, HMM, and SVM. Each of these methods along with all the details of the experimentation is discussed in details in Section 4. This section provides the results of the experimental study described in Section 4. Section 5.1 will provide the results on detection and Section 5.2 will provide results on the performance of the algorithms regarding the recognition of electronic devices.

### 5.1. DETECTION

For the purpose of this research, detection is defined as the ability of the three methods (PCA, HMM, and SVM) in distinguishing UEEs from noise. This section will discuss the performance of these three methods in detecting UEE signals based on the experimental study discussed in Section 4.

**5.1.1 Principal Components Analysis.** This work proposes PCA as a method for UEE detection. The premise behind this proposal is that, as discussed in Section 4.1, the top PCs of noise should have equal contribution in explaining the variation in the dataset whereas the few top PCs on UEE signal should explain most of the variation in the dataset.

The contribution of top 10 PCs of noise and two devices at three different distance is illustrated on Table 5.1. The first column lists the number of principal components. The next six columns lists the contribution of each of the 10 principal components for two devices at three different distances and the last column lists the same for noise.

It can be observed in Table 5.1 that the top two PCs of both devices at three different distances of 3 feet, 6 feet, and 10 feet explains at least 64% of the variability of the UEE signal. This proportion is less than 22% for the noise signal. The top five principal components of the devices explains at least 80% of the total variation but

PC	D1-3ft	D1-6ft	D1-10ft	D2-3ft	D2-6ft	D2-10ft	Noise
<b>1st</b>	57.15%	49.97%	61.85%	43.68%	83.11%	51.84%	13.04%
<b>2nd</b>	80.23%	73.39%	82.49%	65.97%	88.50%	64.00%	21.64%
<b>3rd</b>	89.24%	85.39%	89.75%	77.16%	93.00%	72.97%	29.05%
<b>4th</b>	95.19%	92.08%	94.93%	84.62%	95.70%	76.92%	34.77%
<b>5th</b>	98.19%	96.36%	97.75%	90.54%	97.04%	80.42%	40.37%
<b>6th</b>	98.87%	97.90%	98.60%	93.61%	97.91%	82.84%	45.75%
<b>7th</b>	99.33%	98.90%	99.31%	95.84%	98.52%	84.62%	50.37%
<b>8th</b>	99.59%	99.35%	99.61%	97.30%	99.01%	86.31%	54.77%
<b>9th</b>	99.72%	99.62%	99.75%	98.25%	99.36%	87.43%	58.69%
<b>10th</b>	99.82%	99.77%	99.84%	98.76%	99.54%	88.49%	62.21%

Table 5.1 Cumulative Contribution of Top 10 Principal Components (PC)

in case of noise, it is less than 50%. Similarly, top ten principal components of the devices explains at least 85% of the variation whereas for noise it is less than 65%.

Table 5.2 further clarifies the contribution of PCs of devices by taking the average of two devices at three different distances and comparing it with the top 10 contribution of PCs of noise. The same information is presented in Figure 5.1. Taking average makes the comparison between contribution of PCs more easier to understand and visualize. Top two PCs of devices contributes 75.76% of variation whereas the contribution is only 13.04% in case of noise. Top five PCs of device contribute 93.38% of variation but top 5 PCs of noise is only 40.37%. If all the top 10 principal components are considered, the contribution for device is 97.50% but it is only 62.21% for noise.

Figures 5.2 through 5.8 illustrates the explained variability in all seven cases in a pareto plot. A pareto chart is a bar plot where a line graph represents the cumulative effect of the bars in the plot [89].

Based on these observations, a decision table is developed as shown in table 5.3 to detect UEE signals from noise signals.

Principal Components	Device (Mean)	Noise
1st	57.93%	13.04%
2nd	75.76%	21.64%
3rd	84.59%	29.05%
4th	89.91%	34.77%
5th	93.38%	40.37%
6th	94.96%	45.75%
7th	96.09%	50.37%
8th	96.86%	54.77%
9th	97.36%	58.69%
10th	97.70%	62.21%

Table 5.2 Average Contribution of Top 10 PCs for Devices and Noise

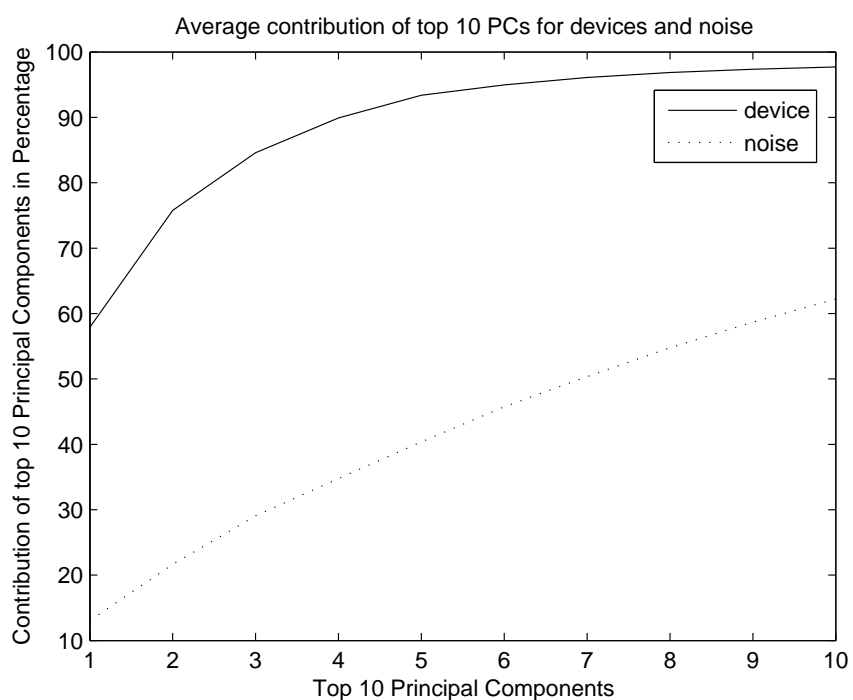


Figure 5.1 Average Contribution of Top 10 PCs for Devices and Noise

No. of Top PC	Total Variation Explained	Results
2	less than 50%	NOISE
2	greater than 50%	UEE
5	less than 75%	NOISE
5	greater than 75%	UEE
10	less than 80%	NOISE
10	greater than 80%	UEE

Table 5.3 Decision Table to Detect UEE

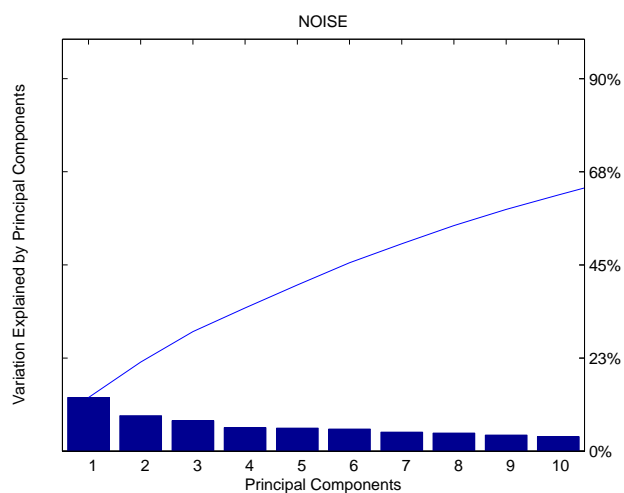


Figure 5.2 Principal Components of Noise

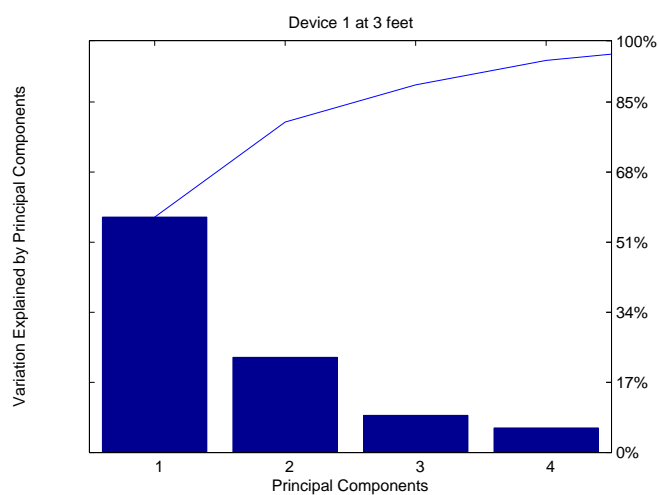


Figure 5.3 Principal Components of Device 1 at 3 feet

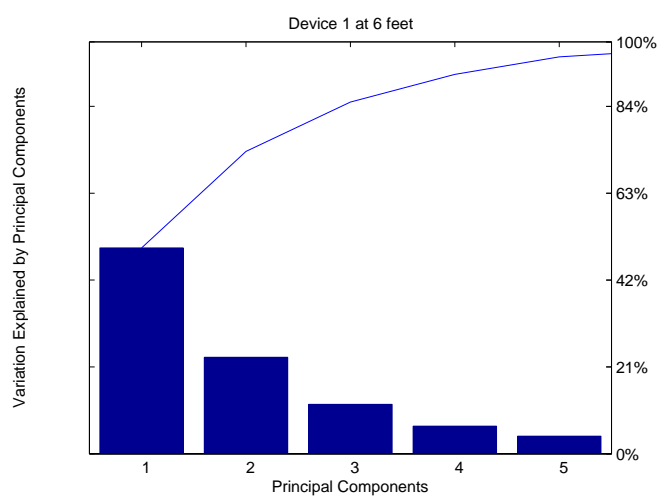


Figure 5.4 Principal Components of Device 1 at 6 feet

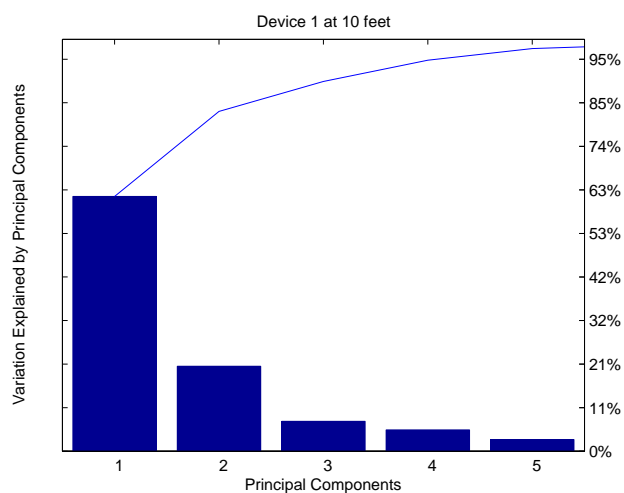


Figure 5.5 Principal Components of Device 1 at 10 feet

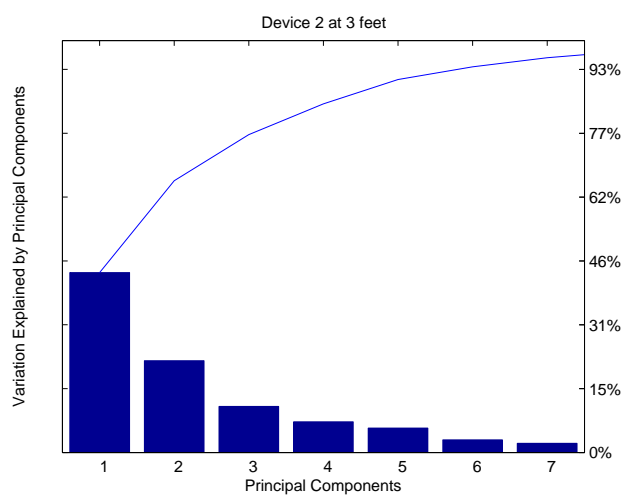


Figure 5.6 Principal Components of Device 2 at 3 feet

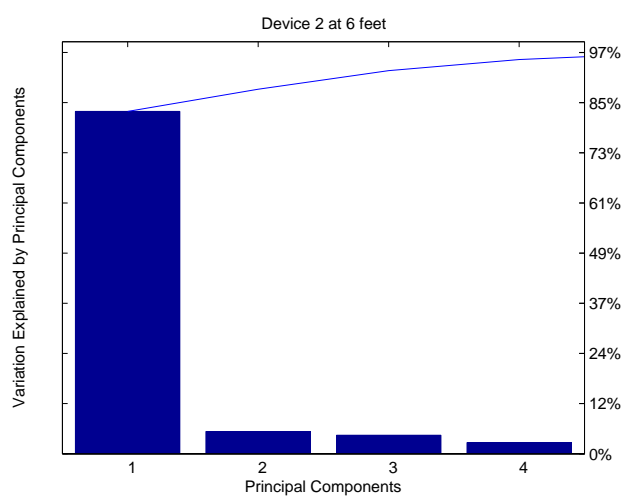


Figure 5.7 Principal Components of Device 2 at 6 feet

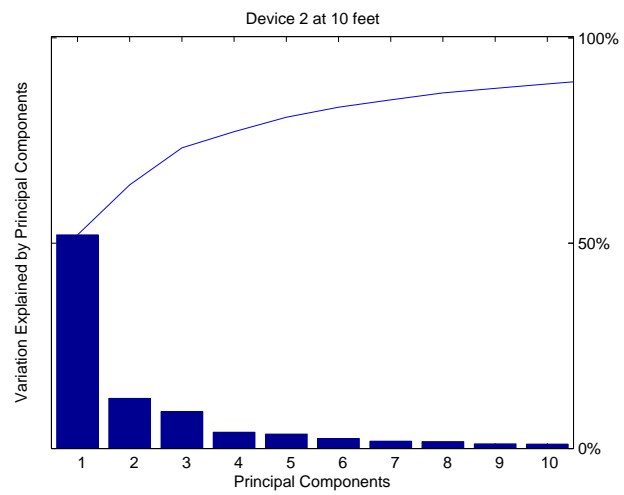


Figure 5.8 Principal Components of Device 2 at 10 feet

**5.1.2 Hidden Markov Models.** Results show that HMM can detect whether there is any electronic device active within a detection range or not. Table 5.4 summarizes the performance of the model in detecting UEEs'. It illustrates the pairwise comparison of noise with each devices at three different distances. The detection rate is 100% for devices at 3 feet but the accuracy decreased to 95% as the distance is increased to 10 feet.

<b>Test Device</b>		
<b>Predicted</b>	Noise	D1-3 feet
Noise	10	0
D1-3 feet	0	10
Accuracy	<b>100%</b>	
<b>Predicted</b>	Noise	D1-6 feet
Noise	10	0
D1-6 feet	0	10
Accuracy	<b>100%</b>	
<b>Predicted</b>	Noise	D1-10 feet
Noise	10	1
D1-10 feet	0	9
Accuracy	<b>95%</b>	
<b>Predicted</b>	Noise	D2-3 feet
Noise	10	0
D2-3 feet	0	10
Accuracy	<b>100%</b>	
<b>Predicted</b>	Noise	D2-6 feet
Noise	10	0
D2-6 feet	0	10
Accuracy	<b>100%</b>	
<b>Predicted</b>	Noise	D2-10 feet
Noise	9	1
D2-10 feet	1	9
Accuracy	<b>90%</b>	

Table 5.4 Device Detection using HMM

The power of UEE is higher when the source of signal is near and the power decreases as the distance increases. As the distance increases, power of UEE decreases and it starts getting buried in the ambient noise. The difference between the noise and UEE signal become less prominent at larger distance. Due to this reason, the

accuracy of HMM in device detection is higher at small distance and the accuracy decreases as the distance increases.

**5.1.3 Support Vector Machine.** SVM gives 100% accuracy in detecting UEEs. The result is illustrated in table 5.5. It was discussed in Section 4.13 that SVM creates a separating hyperplane such that the the margin of separation between noise and UEE is maximized by the separating hyperplane. This means that the boundary that separates noise and UEE is placed exactly in the middle between the two classes. Hence any test signals are more likely to be classified correctly resulting in high detection accuracy.

<b>Test Device</b>		
<b>Predicted</b>	Noise	D1 at 3 feet
Noise	10	0
D1 at 3 feet	0	10
Accuracy	<b>100%</b>	
<b>Predicted</b>	Noise	D1 at 6 feet
Noise	10	0
D1 at 6 feet	0	10
Accuracy	<b>100%</b>	
<b>Predicted</b>	Noise	D1 at 10 feet
Noise	10	0
D1 at 10 feet	0	10
Accuracy	<b>100%</b>	
<b>Predicted</b>	Noise	D1 at 3 feet
Noise	10	0
D2 at 3 feet	0	10
Accuracy	<b>100%</b>	
<b>Predicted</b>	Noise	D2 at 6 feet
Noise	10	0
D2 at 6 feet	0	10
Accuracy	<b>100%</b>	
<b>Predicted</b>	Noise	D2 at 10 feet
Noise	10	0
D2 at 10 feet	0	10
Accuracy	<b>100%</b>	

Table 5.5 Device Detection using SVM

<b>Test Device</b>		
<b>Predicted</b>	Noise	D1 at 3 feet
Noise	10	0
D1 at 3 feet	0	10
Accuracy	<b>100%</b>	
<b>Predicted</b>	Noise	D1 at 6 feet
Noise	10	0
D1 at 6 feet	0	10
Accuracy	<b>100%</b>	
<b>Predicted</b>	Noise	D1 at 10 feet
Noise	10	0
D1 at 10 feet	0	10
Accuracy	<b>100%</b>	
<b>Predicted</b>	Noise	D1 at 3 feet
Noise	10	0
D2 at 3 feet	0	10
Accuracy	<b>100%</b>	
<b>Predicted</b>	Noise	D2 at 6 feet
Noise	10	0
D2 at 6 feet	0	10
Accuracy	<b>100%</b>	
<b>Predicted</b>	Noise	D2 at 10 feet
Noise	10	0
D2 at 10 feet	0	10
Accuracy	<b>100%</b>	

Table 5.6 Device Detection using NN

**5.1.4 Neural Networks.** NNs are the only passive detection technique currently available in literature that is capable of both detecting and recognizing two or more sources of UEEs. Hence NN was selected as the model that will be used for comparing the results of proposed algorithms of this research for the purpose of validation. The performance of Neural Network in detecting UEEs is illustrated in table 5.6. We can observe in table 5.6 that the accuracy of NN in detecting UEEs is 100%.

## 5.2. RECOGNITION

For the purpose of this research, recognition is defined as the ability of the three methods (PCA, HMM, and SVM) in recognizing and differentiating UEEs

from two different RF devices. This section will discuss the performance of these three methods in recognizing UEE signals from two different sources based on the experimental study discussed in Section 4.

**5.2.1 Principal Components Analysis.** Results of PCA analysis on Section 5.1.1 showed that top PCs of UEE explain most of the variation in the dataset but in case of noise, top PCs represent comparatively less variation in the dataset as compared with UEEs. This property was used to differentiate UEE signal from the ambient noise. But if we closely observe the PCs on all devices, there is no pattern in the PCs of devices that will help us differentiate UEE sources from two different devices.

PCs	D1 - 3ft	D2 - 3ft	D1 - 6ft	D2 - 6ft	D1 - 10ft	D2 - 10ft
<b>2</b>	80.23%	65.97%	73.39%	88.50%	82.49%	64.00%
<b>5</b>	98.19%	90.54%	96.36%	97.04%	97.75%	80.42%
<b>10</b>	99.82%	98.76%	99.77%	99.54%	99.84%	88.49%

Table 5.7 Total Variation Explained by top 2, 5, and 10 PCs of Two Devices

Table 5.7 illustrates the total variation explained by top 2, top 5, and top 10 PCs of two devices. At 3 feet, the contribution of PCs of D1 is greater than the contribution of PCs of device D2 for all the three cases (i.e. top 2, top 5, and top 10 PCs). At 6 feet, the situation is reversed and the the contribution of PCs of D2 is greater than the contribution of PCs of device D1 for all the three cases. The results at 10 feet is similar to the results at 3 feet such that the contribution of PCs of D1 is greater than the contribution of PCs of device D2. These results shows that there is no consistent pattern on the contribution of PCs of devices that can be used to distinguish UEE from one device to another.

**5.2.2 Hidden Markov Models.** HMM can not only detect if there is a source of UEE present at a particular distance, but can also recognize between two

sources of UEEs. The performance of HMM in recognizing UEE is illustrated in table 5.8. The recognition accuracy is 90% at 3 feet but the accuracy decreases as the distance increases.

<b>Predicted</b>	D1 at 3 feet	D2 at 3 feet
D1 at 3 feet	8	0
D2 at 3 feet	2	10
Accuracy	<b>90%</b>	
<b>Predicted</b>	D1 at 6 feet	D2 at 6 feet
D1 at 6 feet	5	1
D2 at 6 feet	5	9
Accuracy	<b>70%</b>	
<b>Predicted</b>	D1 at 10 feet	D2 at 10 feet
D1 at 10 feet	8	2
D2 at 10 feet	2	8
Accuracy	<b>80%</b>	

Table 5.8 Device Recognition using HMM

<b>Test Device</b>		
<b>Predicted</b>	D1 at 3 feet	D2 at 3 feet
D1 at 3 feet	10	0
D2 at 3 feet	0	10
Accuracy	<b>100%</b>	
<b>Predicted</b>	D1 at 6 feet	D2 at 6 feet
D1 at 6 feet	10	0
D2 at 6 feet	0	10
Accuracy	<b>100%</b>	
<b>Predicted</b>	D1 at 10 feet	D2 at 10 feet
D1 at 10 feet	10	1
D2 at 10 feet	0	9
Accuracy	<b>95%</b>	

Table 5.9 Device Recognition using SVM

**5.2.3 Support Vector Machine.** Pairwise comparison was performed between D1 and D2 at 3 feet, 6 feet, and 10 feet. The result is presented in Table 5.9.

<b>Test Device</b>		
<b>Predicted</b>	D1 at 3 feet	D2 at 3 feet
D1 at 3 feet	10	0
D2 at 3 feet	0	10
Accuracy	<b>100%</b>	
<b>Predicted</b>	D1 at 6 feet	D2 at 6 feet
D1 at 6 feet	8	1
D2 at 6 feet	2	9
Accuracy	<b>85%</b>	
<b>Predicted</b>	D1 at 10 feet	D2 at 10 feet
D1 at 10 feet	9	1
D2 at 10 feet	1	9
Accuracy	<b>90%</b>	

Table 5.10 Device Recognition using NN

We can observe in table 2 that SVM can accurately identify between two devices at three different distances. Pairwise comparison showed that the accuracy is 100% at 3 feet and 6 feet, and the accuracy is 95% at 10 feet. The decrease in accuracy can be explained by the fact that the signal strength of the UEE decreases as the distance between the devices emitting the signal increases.

**5.2.4 Neural Networks.** The performance of NNs in recognizing between two sources of UEEs at three different distances is illustrated in Table 5.10. The accuracy is 100% at 3 feet and it decreases to 85% and 90% as the distance increases to 6 feet and 10 feet respectively. The accuracy of NNs is greater than the accuracy of HMM but is equal with the accuracy of SVM in detecting UEEs. NNs and SVM gave equal accuracy for detection, but the accuracy of SVM is greater than the accuracy of NNs for recognition.

## 6. CONCLUSION AND FUTURE WORKS

Current methods for detecting UEEs can be divided into two types: stimulated detection and passive detection. Stimulated Detection is the method of detection of UEEs where the underlying characteristics of UEE is strengthened and stabilized by an external stimulation signal. The UEEs in the passive detection methods are not tampered with and are analyzed in its raw form. Stimulated detection methods suffers from the following disadvantages:

1. Stimulated detection methods have only been used for detection, and not for identification of devices
2. There is a work overload of creating and emitting the stimuli signals
3. Extensive characterization measurements of the target devices are required
4. Sometimes, there is a risk that the stimuli signal will interact with the device with unwanted consequences. For example in IED detection, there is a risk that the stimuli signal might detonate the explosive

Passive detection methods don't suffer from these disadvantages, except the third one where characterization of device is required to create the threshold value that is used for deciding if the signal is UEE or noise. The challenge lies in the fact that UEEs are low in power and are often buried deep in the noise band. This research studied the performance of three methods, namely, PCA, HMM, and SVM in the passive detection and recognition of UEEs.

It has been illustrated in Section 5 that PCA can be used to detect UEE from noise but cannot be used to differentiate between two sources of UEE. The reason for this is that the contribution of top PCs of UEE explain most of the variation in data whereas top PCs of noise explain less variation in data. Based on this information, a decision table can be made as illustrated in Section 5.3 that can be used for UEE detection.

It was found that PCA is not capable of differentiating two sources of UEE. The difference between the PCs of UEEs from two devices is not large enough such that top PCs of one device could give extra information from the top PCs of another device. The PCs of two devices at 3 feet, 6 feet, and 10 feet are similar with each other and there is no specific pattern that can differentiate between two similar sources of UEEs.

HMMs can be used for both detection and recognition of UEEs. The accuracy of HMM decreased as the distance of the source of UEE increased. The magnitude of this decrease in accuracy was lower in device detection but considerably higher for device recognition. As illustrated in Figure 4.11, both the detection and recognition are performed by comparing the probability of a particular test signal being emitted by a HMM. Comparison of the probability is made and the device (or noise) that gives the greater probability is chosen. The difference in probabilities of the test signal between noise and UEE has a larger margin than the difference in probabilities between two UEE signal. As the margin of difference in the probability value is small, it is more likely that an incorrect HMM will be selected when comparing the UEEs from two devices. Due to this reason, the accuracy of HMM decreases significantly during device recognition but performs satisfactorily for device detection.

The accuracy of NNs is greater than the accuracy of HMM but is equal with the accuracy of SVM in detecting UEEs. There exists a significant differences between noise and UEE signal for these two algorithm to create a boundary of separation that perfectly separates UEE signal from noise. But in the case of recognizing between two sources of UEE, SVM gave better performance than NNs. UEEs from two devices are very similar with one another. The differences in the characteristics of UEE signals from two devices is very small as compared to the differences in the characteristics of noise and UEE signal. When the difference in characteristic is larger, then the separating hyperplane created by NN was good enough to correctly classify two two classes of noise and UEE signal. In case of UEE signal from two devices, the separating hyperplane of NNs may misclassify few data points as the separating hyperplane of NNs are not optimal. But SVM creates an optimal hyperplane between

the boundary of UEE signal from two devices. Due to this reason, the accuracy of SVM is greater than the accuracy of NNs.

This research has advanced the field of passive detection and recognition methods of UEE. Most of the current focus on UEE is on the costly stimulated detection methods. This research has shown that less costly passive detection methods can be used for UEE detection at short distances. Moreover, most of the current methods for UEE detection cannot separate between two sources of UEEs. The methods explored in this research, with the exception of PCA, can not only detect but also identify and recognize between two sources of UEEs.

The major limitation of this research is that the UEE data is just for two devices and the UEEs are collected only for three different distances. It would be interesting to study the performance of the methods employed in this research to a wide range of RF devices such as cell phones and remote control devices including car key and garage door openers. As the basic characteristics of UEEs are similar, the methodology proposed in this research should be able to detect other RF devices. The only difference will be in determining the bandwidth where consistent UEEs are produced for those devices. The training and testing procedure will be the same.

The decision table proposed in Section 5.3 can be constructed with more accuracy if data from many devices are available with large number of observations. Moreover, if data can be collected for a larger number of distances rather than just three distances of 3 feet, 6 feet, and 10 feet, a thorough investigation can be performed to determine the relationship between distance of UEE source and the accuracy of each method. It will also enable to determine the critical distance for each method beyond which the accuracy decreases significantly and a particular method should not be used for detection and recognition of UEEs.

The military has a need for an effective IED detection system. An IED detection system should perform the task of detection, localization, and the direction of the malicious devices. This research was focused on the detection aspect of IED detection system. It contributed to the IED detection system by proposing stochastic and computational intelligence methods that can not only detect but also recog-

nize between two sources of UEEs. Recognition ability enhances the performance of UEE detection system by providing it with the capability of differentiating malicious sources of UEEs from the ones that are not malicious. NN is the only current passive detection method that has recognition capability. This research also contributed to the passive detection methods of UEE by proposing the application of HMM and SVM, where SVM using radial basis function showed a better performance. Another contribution of this research is in the application of PCA for UEE detection based on the differences between contribution of top principal components of UEE signal and noise.

The first natural extension to this work is to conduct applied research to implement the IED detection system in a real world scenario. It would consist of implementing the methods proposed in this research in relevant hardware and conduct IED detection and recognition by collecting the leakage of electromagnetic signals from RF devices in the form of UEEs. Another immediate extension to this research would be to apply the three proposed algorithms for stimulated detection method. Stimulated detection is nothing but increasing the intensity of the signal so that it would be easier to detect the signal in the ambient noise. Detection and recognition still has to be performed on the stimulated emission. This work will not only increase the detection and recognition range, but will also increase the accuracy.

This research was focussed on the passive detection of low power signals. An additional future work might be the study of performance of algorithms employed in this research to detect and identify low power electromagnetic signals other than UEEs.

## **APPENDIX A**

### **A. Matlab Code for UEE Data Processing**

## Matlab Code for UEE Data Processing

*%% This MATLAB program takes 40 text files of Unintended  
Electromagnetic Emissions*

*%% as input, and performs the data processing tasks for HMM*

**close all;**

**clear all;**

**clc;**

warning off;

*% Defining no of data sets to be used for training in Baum-  
Welch*

no\_train\_set = 30; *% training set for Baum Welch*

*% Defining the number of training set*

no\_training\_set = 30; *% Training set for estimating TPM and EPM*

*% Defining variables for overlap and window size*

w\_size = 100; *% Window Size*

overlap = 50; *% Overlap Size*

*% Counter for intializing the windows*

cWindow = 1;

*% defining range for windows for estimation*

rangeWindows = 9:11;

rangeForWindow = **max**(rangeWindows) - **min**(rangeWindows) + 1;

```

%defining threshold for the purpose of calculating the
%number of peaks in each window
threshold = 1.0e-011 *0.1;
%%%%

%%%%
%Classification criteria for states for the average power for
each of the
%central 3 windows where we have UEE
no_states = 4;
no_observations = 5;

%intializing two cell arrays to store data in dB in watts%
cell_dataWatt=cell(1,40);
cell_dataDb = cell(1,40);

%intializing two cell arrays to dynamically store data in dB
in watts%
dataDb=[];
dataWatt=[];

%To get all the dB data files in matlab workspace
%Please remember that there should be 40 text files on the
same folder as
%this matlab code
for i=1:40
    s=['load_d' int2str(i) '.txt'];
    eval(s);

```

**end;**

*%Importing data from workspace into the cell array for power  
in dB*

**for** i=1:40;

cell\_dataDb{i} = importdata(**sprintf**('d%d.txt',i));

**end**

*%Converting data from dB to watt by importing it first into  
% separate array. After that storing it to array of watts and  
putting it*

*% into cell array for watts*

**for** p=1:40;

dataDb=cell\_dataDb{p};

**for** q=1:**length**(dataDb);

dataWatt(q) =  $10^{((\text{dataDb}(q)-30)/10)}$ ;

**end**

cell\_dataWatt{p}=dataWatt;

**end**

*%defining array for dynamic assignment of windows from 1001*

*data points*

dataWindow = [];

data\_cell\_window = [];

*%Creating windows for each dataset and putting those windows  
in the cell*

*%array created for windows*

*%Define one cell array for windows*

```

cell_window = cell(40,1001);

%Access the first dataset from cell of arrays of power in
watts
%i.e. cell_watt and intialize the first window for first
dataset
%i.e. cell_watt{1}
dataWatt = cell_dataWatt{1};
cell_window{1,1}= dataWatt(1:w_size);
q=w_size;
s=1;
while s<=40;

%Intializing with first window
dataWatt = cell_dataWatt{s};
    cell_window{s,1} = dataWatt(1:w_size);
    %Defining counter for while loop

    %intializing counter for entering into the inner while
    loop to create
    %19 windows for each 48 data sets
    counter = 1;

    %re intializing q to window size for entering into the
    inner while loop to create
    % 19 windows for each 48 data sets
    q=w_size;

```

```

%reintializing cWindow so that it start creating the
window form 2
%through 19 for each data set. first window is already
intialized above
%these intializations
cWindow = 1;

%enter the while loop if counter if counter and q is
less than 952
while(counter < length(dataWatt) + 1 - overlap) && (q < length(
dataWatt)+1 - overlap)

%incrementing counter by 50 i.e. overlap
counter=counter+overlap;

%incrementing q by 50 i.e. overlap
q=q+overlap;

%incrementing cWindow by 1 to create 19 windows
cWindow=cWindow+1;

%putting data from dataWatt to each window
cell_window{s,cWindow}= dataWatt(counter:q);

end;

%incrementing s by 1
s=s+1;

```

```

end;

%calculating the maximum size of cell array to store data in
    psd format
p_size = (max(rangeWindows));

%defining the cell array to store psd data
cell_avg_psd=cell(1,p_size);
cell_peak_psd=cell(1,p_size);

%defining an array for the data manipulation form watt to psd
    format
dataAvgPsd=[];
dataPeakPsd=[];

%running two for loops. Outer loop for each 40 files
%inner for loop for windows in the range defined above
for i=1:40
    for j=min(rangeWindows):max(rangeWindows)
        %converting data from watt to dspdata format
        dataAvgPsd=dspdata.psd(cell_window{i,j});
        %calculating the average of each window
        cell_avg_psd{i,j}=avgpower(dataAvgPsd)*10^12;

        %calculating the no of peaks for each window above
            threshold
        cell_peak_psd{i,j} = numel(findpeaks(dataAvgPsd, '
            minpeakheight', threshold));
    end
end

```

```

        %ending the inner for loop
    end
    %ending outr for loop
end;

%Defining an array for intermidiate operations to append data
avg_pow = [];
no_peak_win = [];
for i=1:no_training_set
    for j=min(rangeWindows):max(rangeWindows)
        avg_pow_append = cell_avg_psd{i,j};
        avg_pow = [avg_pow; avg_pow_append];

        peak_pow_append = cell_peak_psd{i,j};
        no_peak_win = [no_peak_win; peak_pow_append];

    end;
end;
end;

```

## **APPENDIX B**

### **B. Matlab Code for PCA calucation of UEEs**

### Matlab Code for PCA calculation of UEEs

```

%loading UEE data
mydatada = load(ueedata);

%converting the data from cell array format to array format
mynewdata = cell2mat(mydatada);

%reshaping and taking transpose
mynewdata1 = reshape(mynewdata, 400, 40);
mynewdata1 = mynewdata1';

%performing the principal components using the Matlab
function princomp
[pc, score, latent] = princomp(mynewdata1);

%printing the contribution of top 10 principal components
lm = cumsum(latent)./sum(latent);
lm(1:10);

%plotting the principal components
pareto(latent)
principalname = {'1st', '2nd', '3rd', '4th', '5th', '6th', '7
    th', '8th', '9th', '10th'};
xlabel('Principal_Components');
ylabel('Variation_Explained_by_Principal_Components');
title('Device_1_at_3_feet');

```

## APPENDIX C

### C. R code for Baum Welch algorithm

## R code for Baum Welch algorithm

```
# This R program computes the Baum–Welch Algorithm using RHmm
  package

#load sw3 datawatt training data
myndata_trainsw3 <- read.table("sw3_avgpower_400_train.txt")
myndata_trainsw3 <- as.list(myndata_trainsw3)

#fit the data with Baum Welch
sw3hmm <- HMMFit(myndata_trainsw3, nStates = 2)

#load sw3 testing data
myndata_testsw3 <- read.table("sw3_avgpower_400_test.txt")
myndata_testsw3 <- as.list(myndata_testsw3)

# calculate the Viterbi path
VitPathsw3 <- viterbi(sw3hmm, myndata_testsw3)
VitPathsw3$logProbSeq
```

## APPENDIX D

### D. R code for Support Vector Machine

## R code for Support Vector Machine

```
# R program for SVM using e1071 package

require(e1071)
require(R.matlab)

# import data in R
bw3 <- readMat("comprehensive_data_bw30_.mat")
bw3 <- bw3[1]
sw3 <- readMat("comprehensive_data_sw30_.mat")
sw3 <- sw3[1]

#convert list data to data frame
dbw3 <- data.frame(matrix(unlist(bw3), nrow=40, byrow=T))
dsw3 <- data.frame(matrix(unlist(sw3), nrow=40, byrow=T))

# adding label to data set
dbw3$label <- 'bw3'
dsw3$label <- 'sw3'

# merge data frame using 'merge'

traindbw3 <- dbw3[1:30,]
testdbw3 <- dbw3[31:40,]
traindsw3 <- dsw3[1:30,]
testdsw3 <- dsw3[31:40,]

# combining training data and test data
```

```
trainlabelall <- rbind(traindbw3, traindsw3)
testlabelall <- rbind(testdbw3, testdsw3)

# separating the class label from train data
traindata <- subset(trainlabelall, select = -label)
#trainlabel <- subset(trainlabelall, select = label)
trainlabel <- trainlabelall[1:60, 7]

# separating the class label from test data
testdata <- subset(testlabelall, select = -label)
#testlabel <- subset(testlabelall, select = label)
testlabel <- testlabelall[1:20, 7]

# converting training and testing label to factor from data
  frame
trainlabel <- as.factor(trainlabel)
testlabel <- as.factor(testlabel)

# training the svm
mysvm <- svm(traindata, trainlabel)

#testing the support vector machine
pred <- predict(mysvm, testdata)

#check the accuracy of the model
table(pred, testlabel)
```

## **APPENDIX E**

**E. Data segment for D1 at 3 feet**

**Data segment for D1 at 3 feet**

Center Frequency (Hz)	Span (Hz)
441011140	20000

TraceA

-96.18

-98.14

-98.64

-97.69

-96.8

-96.14

-94.93

-93.46

-92.57

-92.74

-94.05

-95.82

-95.82

-95.74

-93.94

-92.34

-92.54

-96.23

-95.35

-92.16

-90.27

-90.61

-93.72

## APPENDIX F

F. Data segment for D1 at 6 feet

**Data segment for D1 at 6 feet**

Center Frequency (Hz)	Span (Hz)
441011140	20000

TraceA

-95.08

-95.82

-100.56

-100.25

-97.04

-95.12

-95.33

-97.53

-100.3

-101.18

-100.69

-100.06

-100.06

-98.85

-96.51

-94.12

-92.72

-92.96

-95.44

-100.89

-103.18

-103.16

-105.95

## APPENDIX G

G. Data segment for D1 at 10 feet

**Data segment for D1 at 10 feet**

Center Frequency (Hz)	Span (Hz)
441011140	20000

TraceA

-96.31

-97.97

-100.28

-102.97

-104.32

-103.16

-101.56

-100.07

-99

-98.55

-97.66

-96.67

-96.67

-97.61

-102.73

-100.21

-97.19

-96.23

-97.05

-96.48

-94.59

-93.17

-92.62

## APPENDIX H

H. Data segment for D2 at 3 feet

**Data segment for D2 at 3 feet**

Center Frequency (Hz)	Span (Hz)
438225064.7	20000

TraceA

-96.7  
-95.04  
-94.2  
-94.77  
-98.34  
-103.32  
-99.84  
-96.03  
-93.57  
-93.19  
-95  
-97.18  
-97.18  
-99.72  
-101.87  
-99.85  
-95.64  
-92.21  
-91.35  
-95.07  
-99.79  
-96.12  
-92.07

## APPENDIX I

### I. Data segment for D2 at 6 feet

**Data segment for D2 at 6 feet**

Center Frequency (Hz)	Span (Hz)
438225064.7	20000

TraceA

-97.28

-94.53

-93.1

-92.96

-94.7

-99.96

-103.21

-101.13

-97.99

-94.62

-92.16

-91.44

-91.44

-92.46

-93.11

-92.03

-90.63

-90.09

-91.55

-100.54

-95.39

-89.71

-85.98

## APPENDIX J

J. Data segment for D2 at 10 feet

## Data segment for D2 at 10 feet

Center Frequency (Hz)	Span (Hz)
438225064.7	20000

TraceA

-107.49

-105.67

-104.19

-104.33

-103.38

-101.12

-98.86

-97.84

-98.13

-97.82

-96.97

-96.89

-96.89

-97.43

-98.36

-99.24

-96.67

-93.86

-92.78

-93.84

-93.77

-91.24

-88.55

## APPENDIX K

### K. Data segment for Noise

**Data segment for Noise**

Center Frequency (Hz)	Span (Hz)
438225064.7	20000

TraceA

-102.97

-102.23

-102.23

-102.6

-102.6

-104.64

-104.64

-108.13

-110.22

-110.22

-109.48

-109.48

-107.49

-107.49

-105.37

-102.98

-102.98

-100.45

-100.45

-98.54

-98.54

-97.84

-98.69

## BIBLIOGRAPHY

- [1] Mobile cellular subscriptions (per 100 people). The World Bank. [Online]. Available: <http://data.worldbank.org/indicator/IT.CEL.SETS.P2> (July 14, 2014)
- [2] N. Bulusu, J. Heidemann, and D. Estrin, "Gps-less low-cost outdoor localization for very small devices," *Personal Communications, IEEE*, vol. 7, no. 5, pp. 28–34, 2000.
- [3] W. McClay and T. McAllister, *Why Place Matters: Geography, Identity, and Civic Life in Modern America*. Encounter Books, 2014.
- [4] The economic benefits of commercial gps use in the united states. NDP Consulting. [Online]. Available: <http://www.gps.gov/governance/advisory/meetings/2012-08/pham.pdf> (August 11, 2014)
- [5] C. S. Miner, D. M. Chan, and C. Campbell. "Digital jewelry: wearable technology for everyday life." *CHI'01 extended abstracts on Human factors in computing systems. ACM*, pp. 45–46, 2001.
- [6] J. Jolly. Tech now: Behind wheel of chevy's 4g car. [Online]. Available: <http://www.usatoday.com/story/tech/columnist/2014/03/11/sxsw-chevrolet-4g/6285745/> (March 10, 2014)
- [7] M. Pun, B. Shrestha, G. R. Upadhaya, P. Manandhar, G. Badal, T. Nagatsuka, S. Ninomiya *et al.*, "Wireless networking and filed server in the high himalayas," in *Proc. of, IAALD/AFITA/WCCA 2008, World Conference on Agricultural Information and IT*, pp. 267–274, 2008.
- [8] L. Pinelis, "The application of intelligent transportation systems (its) and information technology systems to disaster response," Ph.D. dissertation, Massachusetts Institute of Technology, 2006.
- [9] A. Ko and H. Y. Lau, "Robot assisted emergency search and rescue system with a wireless sensor network," *International Journal of Advanced Science and Technology*, vol. 3, pp. 69–78, 2009.
- [10] C. Van Westen and R. Soeters, "Remote sensing and geographic information systems for natural disaster management," *Roy, P., van Westen, CJ and P. Cham-pati Ray (Eds.): Natural Disasters and their mitigation. A Remote Sensing and GIS Perspective. Indian Institute of Remote Sensing. National Remote Sensing Agency, India*, pp. 31–76, 2000.
- [11] R. S. Istepanian, E. Jovanov, and Y. Zhang, "Guest editorial introduction to the special section on m-health: Beyond seamless mobility and global wireless health-care connectivity," *Information Technology in Biomedicine, IEEE Transactions on*, vol. 8, no. 4, pp. 405–414, 2004.

- [12] C. Pattichis, E. Kyriacou, S. Voskarides, M. Pattichis, R. Istepanian, and C. N. Schizas, “Wireless telemedicine systems: an overview,” *Antennas and Propagation Magazine, IEEE*, vol. 44, no. 2, pp. 143–153, 2002.
- [13] G. Shobha, R. R. Chittal, and K. Kumar, “Medical applications of wireless networks,” in *Systems and Networks Communications, 2007. ICSNC 2007. Second International Conference on*. IEEE, pp. 82–82, 2007.
- [14] E. Campo and M. Chan, “Detecting abnormal behaviour by real-time monitoring of patients,” in *Proceedings of the AAAI-02 Workshop Automation as Caregiver*, pp. 8–12, 2002.
- [15] N. Leitgeb, J. Schröttner, and M. Böhm, “Does electromagnetic pollution cause illness?” *Wiener Medizinische Wochenschrift*, vol. 155, no. 9-10, pp. 237–241, 2005.
- [16] V. S. Benson, K. Pirie, J. Schüz, G. K. Reeves, V. Beral, J. Green *et al.*, “Mobile phone use and risk of brain neoplasms and other cancers: prospective study,” *International journal of epidemiology*, p. dyt072, 2013.
- [17] M. H. Repacholi, “Low-level exposure to radiofrequency electromagnetic fields: Health effects and research needs,” *Bioelectromagnetics*, vol. 19, no. 1, pp. 1–19, 1998.
- [18] A. Balmori, “The incidence of electromagnetic pollution on the amphibian decline: Is this an important piece of the puzzle?” *Toxicological & Environmental Chemistry*, vol. 88, no. 2, pp. 287–299, 2006.
- [19] M. K. Irmak, E. Fadilloğlu, M. Güleç, H. Erdoğan, M. Yağmurca, and Ö. Akyol, “Effects of electromagnetic radiation from a cellular telephone on the oxidant and antioxidant levels in rabbits,” *Cell biochemistry and function*, vol. 20, no. 4, pp. 279–283, 2002.
- [20] N. Das, D. Khastgir, T. Chaki, and A. Chakraborty, “Electromagnetic interference shielding effectiveness of carbon black and carbon fibre filled eva and nr based composites,” *Composites part A: applied science and manufacturing*, vol. 31, no. 10, pp. 1069–1081, 2000.
- [21] P. Vlach, B. Segal, and T. Pavlasek, “The measured and predicted electromagnetic environment at urban hospitals,” in *Electromagnetic Compatibility, 1995. Symposium Record., 1995 IEEE International Symposium on*. IEEE, 1995, pp. 4–7.
- [22] J. Schonwalder, M. Fouquet, G. D. Rodosek, and I. Hochstatter, “Future internet= content+ services+ management,” *Communications Magazine, IEEE*, vol. 47, no. 7, pp. 27–33, 2009.
- [23] S. L. Pinski and R. G. Trohman, “Interference with cardiac pacing,” *Cardiology clinics*, vol. 18, no. 1, pp. 219–239, 2000.
- [24] V. Barbaro, P. Bartolini, G. Calcagnini, F. Censi, B. Beard, P. Ruggera, and D. Witters, “On the mechanisms of interference between mobile phones and pacemakers: parasitic demodulation of gsm signal by the sensing amplifier,” *Physics in medicine and biology*, vol. 48, no. 11, pp. 1661, 2003.

- [25] G. V. Tryon, "Millimeter wave case study of operational deployments: retail, airport, military, courthouse, and customs," in *SPIE Defense and Security Symposium*. International Society for Optics and Photonics, 2008, pp. 694 802–694 802.
- [26] C. Johns, R. A. Shellie, O. G. Potter, J. W. O'Reilly, J. P. Hutchinson, R. M. Guijt, M. C. Breadmore, E. F. Hilder, G. W. Dicoski, and P. R. Haddad, "Identification of homemade inorganic explosives by ion chromatographic analysis of post-blast residues," *Journal of Chromatography A*, vol. 1182, no. 2, pp. 205–214, 2008.
- [27] Ied device. Wikimedia Commons. [Online]. Available: [http://commons.wikimedia.org/wiki/File:IED\\_01.jpg](http://commons.wikimedia.org/wiki/File:IED_01.jpg) (April 11, 2012)
- [28] T. Strother, "Cell phone use by insurgents in iraq," *Urban Warfare Analysis Center*, vol. 14, 2007.
- [29] A. Juels, "Rfid security and privacy: A research survey," *Selected Areas in Communications, IEEE Journal on*, vol. 24, no. 2, pp. 381–394, 2006.
- [30] R. Weinstein, "Rfid: a technical overview and its application to the enterprise," *IT professional*, vol. 7, no. 3, pp. 27–33, 2005.
- [31] L. M. Ni, D. Zhang, and M. R. Souryal, "Rfid-based localization and tracking technologies," *Wireless Communications, IEEE*, vol. 18, no. 2, pp. 45–51, 2011.
- [32] S. A. Seguin, "Detection of low cost radio frequency receivers based on their unintended electromagnetic emissions and an active stimulation," *Ph.D. dissertation, Missouri University of Science and Technology*, 2009.
- [33] F. Dowla, *Handbook of RF and wireless technologies*, Newnes Publishing, 2003.
- [34] A. Shaik, H. Weng, X. Dong, T. H. Hubing, and D. G. Beetner, "Matched filter detection and identification of electronic circuits based on their unintentional radiated emissions," in *2006 IEEE International Symposium on Electromagnetic Compatibility*. Institute of Electrical and Electronics Engineers IEEE, 2006.
- [35] M. P. Kennedy, "Chaos in the colpitts oscillator," *Circuits and Systems I: Fundamental Theory and Applications, IEEE Transactions on*, vol. 41, no. 11, pp. 771–774, 1994.
- [36] M. K. Bole, J. McGraw, F. Ryan, T. Hawley, M. Davis, and T. Van, "Integrated passive electronic signature modeling," in *SPIE Defense, Security, and Sensing*. International Society for Optics and Photonics, pp. 73 240Y–73 240Y, 2009.
- [37] H. Sekiguchi and S. Seto, "Proposal of an information signal measurement method in display image contained in electromagnetic noise emanated from a personal computer," in *Instrumentation and Measurement Technology Conference Proceedings, 2008. IMTC 2008. IEEE*. IEEE, pp. 1859–1863, 2008.
- [38] H. Weng, X. Dong, X. Hu, D. Beetner, T. Hubing, and D. Wunsch, Neural network detection and identification of electronic devices based on their unintended emissions, in *Proc. IEEE International Symposium on Electromagnetic Compatibility, Chicago, IL, Aug. 812*, vol. 1, pp. 245–249, 2005.

- [39] V. Thotla, M. T. A. Ghasr, M. Zawodniok, S. Jagannathan, and S. Agarwal, "Detection and localization of r/c electronic devices using hurst parameter," in *SPIE Defense, Security, and Sensing*. International Society for Optics and Photonics, pp. 835 915–835 915, 2012.
- [40] B. Wild and K. Ramchandran, "Detecting primary receivers for cognitive radio applications," in *New Frontiers in Dynamic Spectrum Access Networks, 2005. DySPAN 2005. 2005 First IEEE International Symposium on*. IEEE, pp. 124–130, 2005.
- [41] C. Stagner, A. Conrad, C. Osterwise, D. G. Beetner, and S. Grant, "A practical superheterodyne-receiver detector using stimulated emissions," *Instrumentation and Measurement, IEEE Transactions on*, vol. 60, no. 4, pp. 1461–1468, 2011.
- [42] S. M. Weiss, R. D. Weller, and S. Driscoll, "New measurements and predictions of uhf television receiver local oscillator radiation interference," *Merrill Weiss Group, Metuchen*, 2006.
- [43] S. K. Subedi, "Experimental investigation of rf fading channels and receiver detection," *Masters Thesis, Missouri University of Science and Technology*, 2012.
- [44] W. Stallings, *Wireless communications & networks*. Pearson Education India, 2009.
- [45] S. Subedi, Z. Wang, and Y. R. Zheng, "Improving detection range via correlation of long pn codes," in *SPIE Defense, Security, and Sensing*. International Society for Optics and Photonics, pp. 835 729–835 729, 2012.
- [46] C. Stagner, A. Conrad, C. Osterwise, D. G. Beetner, and S. Grant, "A practical superheterodyne-receiver detector using stimulated emissions," *Instrumentation and Measurement, IEEE Transactions on*, vol. 60, no. 4, pp. 1461–1468, 2011.
- [47] J. G. Proakis, "Digital communications," McGraw-Hill, New York, 1995.
- [48] R. G. Clegg. (2006) A practical guide to measuring the hurst parameter. <http://arxiv.org/pdf/math.ST/0610756.pdf>.
- [49] J. Hertenstein and S. Jagannathan, "Detection of unintended electromagnetic emissions from super-regenerative receivers," in *SPIE Defense, Security, and Sensing*. International Society for Optics and Photonics, pp. 80 170F–80 170F, 2011.
- [50] F. Serinaldi, "Use and misuse of some hurst parameter estimators applied to stationary and non-stationary financial time series," *Physica A: Statistical Mechanics and its Applications*, vol. 389, no. 14, pp. 2770–2781, 2010.
- [51] I. G. Guardiola and F. Mallor, "A nonparametric method for detecting unintended electromagnetic emissions," *Electromagnetic Compatibility, IEEE Transactions on*, vol. 55, no. 1, pp. 58–65, 2013.
- [52] M. Gastón-Romeo, T. Leon, F. Mallor, and L. Ramírez-Santigosa, "A morphological clustering method for daily solar radiation curves," *Solar Energy*, vol. 85, no. 9, pp. 1824–1836, 2011.

- [53] M. Van der Laan, K. Pollard, and J. Bryan, “A new partitioning around medoids algorithm,” *Journal of Statistical Computation and Simulation*, vol. 73, no. 8, pp. 575–584, 2003.
- [54] H.-S. Park and C.-H. Jun, “A simple and fast algorithm for k-medoids clustering,” *Expert Systems with Applications*, vol. 36, no. 2, pp. 3336–3341, 2009.
- [55] X. Dong, H. Weng, D. G. Beetner, T. H. Hubing, D. C. Wunsch, M. Noll, H. Goksu, and B. Moss, “Detection and identification of vehicles based on their unintended electromagnetic emissions,” *Electromagnetic Compatibility, IEEE Transactions on*, vol. 48, no. 4, pp. 752–759, 2006.
- [56] I. Var, “Multivariate data analysis,” *vectors*, vol. 8, no. 6, 1998.
- [57] J. Rust, “Using randomization to break the curse of dimensionality,” *Econometrica: Journal of the Econometric Society*, pp. 487–516, 1997.
- [58] B. W. Silverman, *Density estimation for statistics and data analysis*. CRC press, vol. 26, 1986.
- [59] G. E. Hinton and R. R. Salakhutdinov, “Reducing the dimensionality of data with neural networks,” *Science*, vol. 313, no. 5786, pp. 504–507, 2006.
- [60] M. Ringnér, “What is principal component analysis?” *Nature biotechnology*, vol. 26, no. 3, pp. 303–304, 2008.
- [61] S. P. Acharya and I. G. Guardiola, “Detection of rf devices based on their unintended electromagnetic emissions using principal components analysis,” in *Wireless Telecommunications Symposium (WTS), 2013*. IEEE, pp. 1–5, 2013.
- [62] J. Shlens. A tutorial on principal component analysis. [Online]. Available: <http://www.cs.cmu.edu/~elaw/papers/pca.pdf> (March 4, 2014)
- [63] O. Vaidya, G. Howell, and D. Leger, “Evaluation of the distribution of mercury in lakes in nova scotia and newfoundland (canada),” *Water, Air, and Soil Pollution*, vol. 117, no. 1-4, pp. 353–369, 2000.
- [64] S. S. Haykin, *Neural networks and learning machines*. Pearson Education Upper Saddle River, vol. 3, 2009.
- [65] J. Dien, “Addressing misallocation of variance in principal components analysis of event-related potentials,” *Brain Topography*, vol. 11, no. 1, pp. 43–55, 1998.
- [66] L. Rabiner, “A tutorial on hidden markov models and selected applications in speech recognition,” *Proceedings of the IEEE*, vol. 77, no. 2, pp. 257–286, 1989.
- [67] S. R. Eddy, “What is a hidden markov model?” *Nature biotechnology*, vol. 22, no. 10, pp. 1315–1316, 2004.
- [68] M. Brand, N. Oliver, and A. Pentland, “Coupled hidden markov models for complex action recognition,” in *Computer Vision and Pattern Recognition, 1997. Proceedings., 1997 IEEE Computer Society Conference on*. IEEE, pp. 994–999, 1997.

- [69] H. Bunke, M. Roth, and E. G. Schukat-Talamazzini, “Off-line cursive handwriting recognition using hidden markov models,” *Pattern recognition*, vol. 28, no. 9, pp. 1399–1413, 1995.
- [70] M. Beyreuther, R. Carniel, and J. Wassermann, “Continuous hidden markov models: application to automatic earthquake detection and classification at las cañadas caldera, tenerife,” *Journal of Volcanology and Geothermal Research*, vol. 176, no. 4, pp. 513–518, 2008.
- [71] A. Kale, A. Sundaresan, A. Rajagopalan, N. P. Cuntoor, A. K. Roy-Chowdhury, V. Kruger, and R. Chellappa, “Identification of humans using gait,” *Image Processing, IEEE Transactions on*, vol. 13, no. 9, pp. 1163–1173, 2004.
- [72] J.-J. J. Lien, “Automatic recognition of facial expressions using hidden markov models and estimation of expression intensity,” Ph.D. dissertation, Washington University, 1998.
- [73] D. K. D. Haussler and M. G. R. F. H. Eeckman, “A generalized hidden markov model for the recognition of human genes in dna,” in *Proc. Int. Conf. on Intelligent Systems for Molecular Biology, St. Louis*, pp. 134–142, 1996.
- [74] L. R. Rabiner and B.-H. Juang., *Fundamentals of speech recognition*, L. R. Rabiner and B.-H. Juang., Eds. Englewood Cliffs: PTR Prentice Hall, 1993.
- [75] M. Beyreuther, C. Hammer, J. Wassermann, M. Ohrnberger, and T. Megies, “Constructing a hidden markov model based earthquake detector: application to induced seismicity,” *Geophysical Journal International*, vol. 189, no. 1, pp. 602–610, 2012.
- [76] U. N. Bhat and G. K. Miller, *Elements of applied stochastic processes*. J. Wiley, 1972.
- [77] J. A. Bilmes, “What hmms can do,” *IEICE TRANSACTIONS on Information and Systems*, vol. 89, no. 3, pp. 869–891, 2006.
- [78] Y.-F. Zhang, Q.-F. Zhang, and R.-H. Yu, “Markov property of markov chains and its test,” in *Machine Learning and Cybernetics (ICMLC), 2010 International Conference on*, vol. 4. IEEE, pp. 1864–1867, 2010.
- [79] B. E. Boser, I. M. Guyon, and V. N. Vapnik, “A training algorithm for optimal margin classifiers,” in *Proceedings of the fifth annual workshop on Computational learning theory*. ACM, pp. 144–152, 1992.
- [80] V. N. Vapnik, “An overview of statistical learning theory,” *Neural Networks, IEEE Transactions on*, vol. 10, no. 5, pp. 988–999, 1999.
- [81] F. Chu, G. Jin, and L. Wang, “Cancer diagnosis and protein secondary structure prediction using support vector machines,” in *Support Vector Machines: Theory and Applications*. Springer, pp. 343–363, 2005.
- [82] T. M. Cover, “Geometrical and statistical properties of systems of linear inequalities with applications in pattern recognition,” *Electronic Computers, IEEE Transactions on*, no. 3, pp. 326–334, 1965.

- [83] M. N. Wernick, Y. Yang, J. G. Brankov, G. Yourganov, and S. C. Strother, "Machine learning in medical imaging," *Signal Processing Magazine, IEEE*, vol. 27, no. 4, pp. 25–38, 2010.
- [84] B. Widrow, D. E. Rumelhart, and M. A. Lehr, "Neural networks: Applications in industry, business and science," *Communications of the ACM*, vol. 37, no. 3, pp. 93–105, 1994.
- [85] S. Ghosh and D. L. Reilly, "Credit card fraud detection with a neural-network," in *System Sciences, 1994. Proceedings of the Twenty-Seventh Hawaii International Conference on*, vol. 3. IEEE, pp. 621–630, 1994.
- [86] D. Enke and S. Thawornwong, "The use of data mining and neural networks for forecasting stock market returns," *Expert Systems with applications*, vol. 29, no. 4, pp. 927–940, 2005.
- [87] M. T. Leung, H. Daouk, and A.-S. Chen, "Forecasting stock indices: a comparison of classification and level estimation models," *International Journal of Forecasting*, vol. 16, no. 2, pp. 173–190, 2000.
- [88] K. Schierholt and C. H. Dagli, "Stock market prediction using different neural network classification architectures," in *Computational Intelligence for Financial Engineering, 1996., Proceedings of the IEEE/IAFE 1996 Conference on*. IEEE, 1996, pp. 72–78.
- [89] L. Wilkinson, "Revising the pareto chart," *The American Statistician*, vol. 60.4, pp. 332–334, 2006.

## VITA

Shikhar Prasad Acharya was born on March 18, 1982 in Kathmandu, Nepal. He received his Bachelor of Engineering degree in Computer Engineering from Kathmandu University, Dhulikhel, Nepal in 2004, his Master of Business Administration in Finance from Ace Institute of Management, Kathmandu, Nepal in 2007 and Doctor of Philosophy degree in Systems Engineering from Missouri University of Science and Technology, Rolla, MO, USA in May 2015. His research interests include application of Statistical and Computational Intelligence methods for data mining, knowledge discovery, and pattern recognition.

Shikhar Prasad Acharya has published his research work in journals and peer reviewed proceedings and has also presented his work in various conferences. Apart from research, he has a keen interest in teaching. He received the outstanding graduate student teaching award for the year 2014. He has a wide range of hobbies including reading, gardening, traveling, movies, and poetry.